Title

Structural basis for activation of trimeric Gi proteins by multiple growth factor receptors via GIV/Girdin

Journal

Molecular Biology of the Cell, 25(22)

ISSN

1059-1524

Authors

Lin, Changsheng
Ear, Jason
Midde, Krishna
et al.

Publication Date

2014-11-05

DOI

10.1091/mbc.e14-05-0978

Peer reviewed

Structural basis for activation of trimeric Gi proteins by multiple growth factor receptors via GIV/Girdin

Changsheng Lin[a,*,†], Jason Ear[a,*,‡], Krishna Midde[a], Inmaculada Lopez-Sanchez[a], Nicolas Aznar[a], Mikel Garcia-Marcos[b,§], Irina Kufareva[c], Ruben Abagyan[c], and Pradipta Ghosh[a]

[a]Department of Medicine and [b]Department of Cellular and Molecular Medicine, University of California, San Diego, School of Medicine, and [c]Skaggs School of Pharmacy and Pharmaceutical Sciences, University of California, San Diego, La Jolla, CA 92093

ABSTRACT **A long-standing issue in the field of signal transduction is to understand the cross-talk between receptor tyrosine kinases (RTKs) and heterotrimeric G proteins, two major and distinct signaling hubs that control eukaryotic cell behavior. Although stimulation of many RTKs leads to activation of trimeric G proteins, the molecular mechanisms behind this phenomenon remain elusive. We discovered a unifying mechanism that allows GIV/Girdin, a bona fide metastasis-related protein and a guanine-nucleotide exchange factor (GEF) for Gαi, to serve as a direct platform for multiple RTKs to activate Gαi proteins. Using a combination of homology modeling, protein–protein interaction, and kinase assays, we demonstrate that a stretch of ~110 amino acids within GIV C-terminus displays structural plasticity that allows folding into a SH2-like domain in the presence of phosphotyrosine ligands. Using protein–protein interaction assays, we demonstrated that both SH2 and GEF domains of GIV are required for the formation of a ligand-activated ternary complex between GIV, Gαi, and growth factor receptors and for activation of Gαi after growth factor stimulation. Expression of a SH2-deficient GIV mutant (Arg 1745→Leu) that cannot bind RTKs impaired all previously demonstrated functions of GIV—Akt enhancement, actin remodeling, and cell migration. The mechanistic and structural insights gained here shed light on the long-standing questions surrounding RTK/G protein cross-talk, set a novel paradigm, and characterize a unique pharmacological target for uncoupling GIV-dependent signaling downstream of multiple oncogenic RTKs.**

Monitoring Editor
Carl-Henrik Heldin
Ludwig Institute for Cancer Research

Received: May 14, 2014
Revised: Jul 25, 2014
Accepted: Aug 22, 2014

INTRODUCTION

Signal transduction pathways link internal and environmental signals to cellular responses. It is well known that various signaling pathways cross-talk at multiple levels to generate large, complex signaling networks that ultimately control cell fate (Liebmann and Bohmer, 2000). In eukaryotes, two widely studied and distinct signaling pathways are the receptor tyrosine kinases (RTKs) and trimeric G proteins.

This article was published online ahead of print in MBoC in Press (http://www.molbiolcell.org/cgi/doi/10.1091/mbc.E14-05-0978) on September 3, 2014.

*These authors contributed equally.

Present addresses: †J. David Gladstone Institute, San Francisco, CA 94158; ‡Department of Molecular, Cell and Developmental Biology, University of California, Los Angeles, Los Angeles, CA 90095; §Department of Biochemistry, Boston University School of Medicine, Boston, MA 02118.

The authors declare that they have no competing financial interests.

C.L., J.E., and P.G. designed, performed, and analyzed most of the experiments. I.K. and R.A. carried out the sequence alignments, built the homology model of GIV-SH2 alone and in complex with EGFR peptide, and made predictions regarding the effect of various mutageneses on GIV:EGFR binding. K.M. validated the various BiFC constructs in vitro and in cells and performed and analyzed the BiFC experiments. I.L.-S. and N.A. performed the cAMP and Gαi:GTP assays, respectively. M.G.-M. performed and analyzed the steady-state GTPase assays and edited the manuscript. P.G. conceived, supervised, and funded the project and wrote the manuscript.

Address correspondence to: Pradipta Ghosh (prghosh@ucsd.edu).

Abbreviations used: EGF, epidermal growth factor; GEF, guanine nucleotide exchange factor; GIV, Gα-interacting vesicle-associated protein; GPCR, G protein–coupled receptor; Ins, insulin; PI3K, phosphoinositide 3 kinase; RTK, receptor tyrosine kinase; SH2, Src homology domain; Shc1, SH2 domain–containing transforming protein 1; SHP-1, SH2-containing protein phosphatase-1.

On binding of growth factors such as epidermal growth factor (EGF) or insulin, RTKs phosphorylate a variety of targets on tyrosines to propagate signals to the cell's interior (Gschwind *et al.*, 2004). Trimeric G proteins, on the other hand, are traditionally defined as molecular switches that transmit signals from a different class of membrane receptors, the seven-transmembrane (7TM) receptors, also known as G protein–coupled receptors (GPCRs; Marinissen and Gutkind, 2001; Mills and Moolenaar, 2003; Luttrell, 2006). These receptors work as guanine nucleotide exchange factors (GEFs), which directly bind and activate the G proteins, which in turn signal via downstream effectors/intermediates.

Despite being distinct pathways, it has been widely demonstrated that the RTK and GPCR/G protein pathways cross-talk (Liebmann and Bohmer, 2000; Lowes *et al.*, 2002; Piiper and Zeuzem, 2004; Natarajan and Berk, 2006). RTKs can be indirectly activated by GPCR/G protein intermediates by so-called transactivation (Daub *et al.*, 1996; Luttrell *et al.*, 1999; Schafer *et al.*, 2004), and, conversely, G proteins may be activated downstream of RTKs (Marty and Ye, 2010). The concept of activation of RTKs by GPCR/G proteins is widely accepted and supported by in-depth mechanistic insights; however, the converse concept, that trimeric G proteins may be activated upon RTK stimulation, remains highly controversial because neither RTKs nor RTK-binding adaptors described to date possess any intrinsic GEF activity toward trimeric G proteins. The lack of concrete mechanistic insights into direct or indirect stimulation of G proteins by RTKs has fuelled speculation (Marty and Ye, 2010) that perhaps RTKs transactivate GPCRs through physical association with G proteins (Sun *et al.*, 1995; Poppleton *et al.*, 1996), phosphorylation of the GPCRs, up-regulation of GPCR-ligand synthesis, or various combinations of these. Despite decades of investigation yielding numerous clues that growth factors can activate heterotrimeric G proteins (Marty and Ye, 2010), the fundamental questions as to how that occurs in cells and what might be the biological significance of such activation remain unanswered.

Besides receptor GEFs, that is, GPCRs, heterotrimeric G-protein signaling can also be activated by nonreceptor GEFs, a rapidly growing family of G protein modulators (Cismowski *et al.*, 2000, 2001; Tall *et al.*, 2003; Garcia-Marcos *et al.*, 2009; Lee and Dohlman, 2008). The Gα-interacting vesicle-associated protein (GIV, also known as Girdin) is a multidomain, nonreceptor GEF for G proteins, Gαi1/2/3 (Garcia-Marcos *et al.*, 2009), which can enhance phosphoinositide 3-kinase (PI3K)/Akt signals, remodel cytoskeleton, and trigger cell migration downstream of multiple ligand-activated RTKs (Ghosh *et al.*, 2011), for example, EGF receptor (EGFR; Enomoto *et al.*, 2005; Ghosh *et al.*, 2008, 2010), insulin-like growth factor 1 receptor (IGF1R; Jiang *et al.*, 2008), vascular endothelial growth factor receptor (VEGFR; Kitamura *et al.*, 2008; Wang *et al.*, 2014), platelet-derived growth factor receptor (Lopez-Sanchez *et al.*, 2014), and insulin R (Garcia-Marcos *et al.*, 2010, 2011a, 2012; Ghosh *et al.*, 2008; Lin *et al.*, 2011). Consistent with its overly promiscuous behavior of being able to partner with multiple receptors/pathways and affect multireceptor signaling, GIV plays major roles in diverse biological processes, including epithelial wound healing (Enomoto *et al.*, 2005; Ghosh *et al.*, 2008), macrophage chemotaxis (Ghosh *et al.*, 2008), development (Puseenam *et al.*, 2009; Yamaguchi *et al.*, 2010), autophagy (Garcia-Marcos *et al.*, 2011a), neuronal migration (Enomoto *et al.*, 2009; Porteous and Millar, 2009; Wang *et al.*, 2011), podocyte survival in nephrotic syndrome (Wang *et al.*, 2014), fibrosis/repair in the injured liver (Lopez-Sanchez *et al.*, 2014), vascular injury and repair (Miyake *et al.*, 2011), tumor neoangiogenesis (Kitamura *et al.*, 2008), tumor cell migration (Enomoto *et al.*, 2005; Jiang *et al.*, 2008; Ghosh *et al.*, 2010), cancer invasion (Jiang *et al.*, 2008), and tumor metastasis (Garcia-Marcos *et al.*, 2011b). Despite the growing evidence, the structural or biochemical basis for how GIV might engage with multiple RTKs and modulate their downstream signals remains a mystery.

Here we show that GIV binds multiple RTKs via a unique C-terminal stretch that reveals sequence-dependent structural plasticity by folding into a Src homology 2 (SH2) module. Thus GIV appears to be the first SH2-like adaptor of its kind to directly couple RTK activation to trimeric G protein activation via its intrinsic GEF activity.

RESULTS

GIV directly binds autophosphorylated cytoplasmic tails of multiple RTKs

We previously demonstrated that GIV is recruited to ligand-activated EGFR (Ghosh *et al.*, 2010). To discern whether GIV can interact directly with multiple ligand-activated RTKs, we tested the ability of the C-terminus of GIV to bind recombinant, autophosphorylated cytoplasmic tails of EGFR, VEGFR, and insulin receptor β (InsRβ) containing their respective kinase domains in pull-down assays. These three RTKs were chosen because we and others have demonstrated that GIV modulates Akt signaling and triggers cell migration when any of these three receptors is activated by its respective ligand (Enomoto *et al.*, 2005; Jiang *et al.*, 2008; Kitamura *et al.*, 2008; Garcia-Marcos *et al.*, 2009, 2010, 2011a, 2012; Ghosh *et al.*, 2010; Lin *et al.*, 2011). We found that a purified ~200–amino acid (aa)–long C-terminal fragment of GIV is sufficient for GIV to bind all three recombinant active RTKs (Figure 1a), demonstrating that GIV can directly bind multiple autophosphorylated RTKs via its C-terminus. Next we asked which autophosphorylated tyrosine on the RTK tail GIV binds. Among the various RTKs, we focused on EGFR for two reasons: 1) it is a prototype RTK, and 2) EGFR autophosphorylation is best characterized, with in-depth understanding of the function of each autophosphorylation site and the signaling intermediates/adaptors that they recruit (Helin *et al.*, 1991; Decker, 1993; Batzer *et al.*, 1994; Okabayashi *et al.*, 1994; Okutani *et al.*, 1994).

On the basis of clues from our previous work (Ghosh *et al.*, 2010), which showed that aa 1020–1210 of the cytoplasmic tail of EGFR are sufficient for binding to GIV-CT, we mapped the phosphotyrosine-binding site for GIV on the EGFR tail by focusing exclusively on four of the five known sites of receptor autophosphorylation—Y1068, Y1086, Y1148, and Y1173—which are present within that stretch of EGFR. Owing to the existence of multiple EGFR isoforms, each with its unique numbering of amino acids, autophosphorylation sites were identified by the sequence flanking the tyrosines (Savage and Cohen, 1972; Margolis *et al.*, 1989; Walton *et al.*, 1990; Sorkin *et al.*, 1991, 1992), and glutathione *S*-transferase (GST)–tagged EGFR tail (EGFR-T) peptides were cloned such that each construct allowed isolated testing of one or two of these four sites of autophosphorylation at a given time (Figure 1b). As a negative control, we also tested another tyrosine, Y1114, which does not get phosphorylated in the intact EGFR either in kinase reactions in vitro or in cells after EGF stimulation (Margolis *et al.*, 1989). These GST-tagged EGFR-T peptides were purified, phosphorylated in in vitro kinase assays using recombinant EGFR kinase (Figure 1c), and subsequently used in pull-down assays with recombinant GIV-CT. We found that GIV interacted exclusively with GST-EGFR-T peptides containing phosphotyrosine Y1148 or Y1173 (Figure 1d), indicating that GIV-CT specifically binds to EGFR peptides containing those two but not the other autophosphorylated (Y1068, and Y1086) or nonphosphorylatable (Y1114) tyrosines. Because purified recombinant proteins were used in these protein–protein interaction assays, we conclude that the interaction between GIV's C-terminus and the

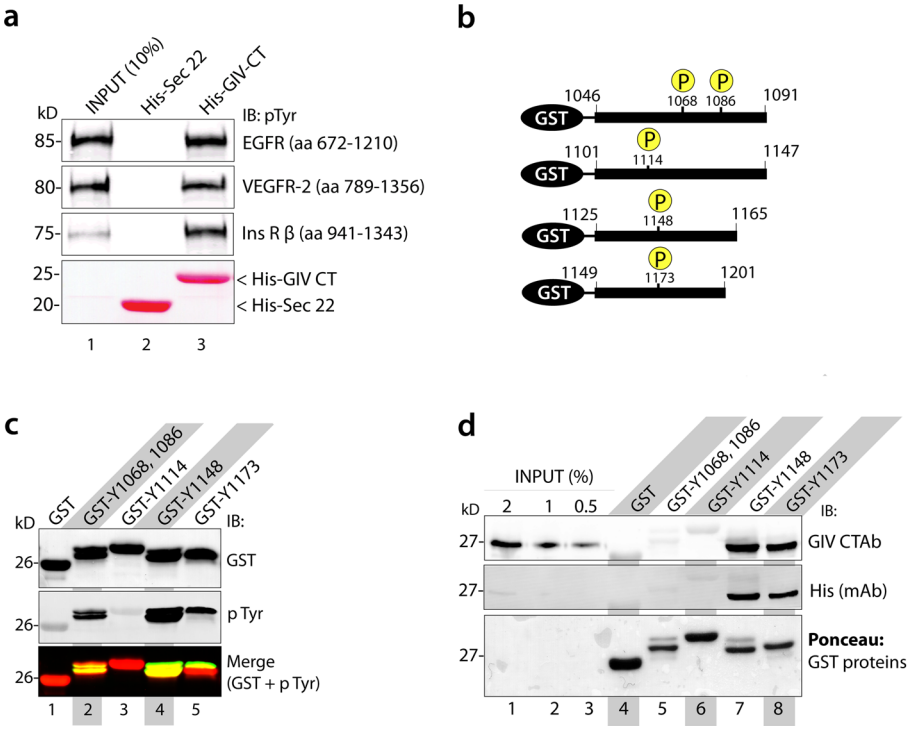

FIGURE 1: The C-terminus of GIV directly binds autophosphorylated cytoplasmic tails of multiple RTKs. (a) Recombinant cytoplasmic tails of EGFR, InsR, and VEGFR were autophosphorylated and subsequently used in binding assays with His-GIV-CT (aa 1660–1870) or His-Sec22 (a negative control) prebound to cobalt beads. Bound proteins were analyzed for His-tagged proteins by Ponceau staining (bottom) and autophosphorylated receptors by IB with anti-pTyr mAb (top). (b) Schematic representation of GST-tagged, phospho–EGFR-tail peptides used in this work. (c, d) Equal aliquots (25 μg) of GST and GST-EGFR peptides containing the indicated tyrosines were autophosphorylated in vitro using recombinant EGFR kinase and subsequently used in pull-down assays with His-GIV-CT as in a. (c) An aliquot of the GST proteins were analyzed for GST and pTyr by IB. Single-channel images for GST and pTyr are displayed in grayscale. Yellow pixels in the overlay images (merge panels) confirm that Y1068, 86, Y1148, and Y1173 are autophosphorylated on tyrosine(s) by EGFR (lanes 2, 4, 5), whereas GST (lane 1) and GST-Y1114 (lane 3) are not. (d) Bound proteins were visualized by IB for His. His-GIV-CT bound strongly to GST-Y1148 (lane 7) and with GST-Y1173 (lane 8) but not to GST alone or other GST-EGFR peptides (lanes 4–6).

two major sites of receptor autophosphorylation on the EGFR tail is direct.

The C-terminus of GIV contains a unique SH2-like domain

Next we examined whether GIV-CT contains any functional domains that might recognize and bind the major autophosphorylation sites on EGFR tail—the SH2 and phosphotyrosine-binding (PTB) domains, two well-characterized and widely studied domains that recognize and bind phosphotyrosines (Schlessinger and Lemmon, 2003). To search systematically for similarities between GIV and other known phosphotyrosine binding domains, we aligned the sequences corresponding to the C-terminal domain of human (BAE44387; aa 1660–1870) and mouse (NP_789811; aa 1600–1845) GIV with other known SH2 and PTB domains in various proteins by pfam alignment using the MolSoft ICM molecular modeling suite (Abagyan *et al.*, 1997; Cardozo *et al.*, 1995, 2000). A stretch of ~110 aa, 1713–1823, of GIV-CT showed weak similarity to the consensus sequence shared by 43 other SH2 domains in various proteins (Supplemental Figure S1), whereas no significant similarity was noted between known PTB domains and GIV. This putative SH2-like stretch in GIV's C-terminus lies ~15 aa downstream of the previously reported GEF motif (Figure 2a). This stretch contains the critical *GXFXXR* motif, which is conserved across all SH2 adaptors, widely implicated in the structural basis for recognition and binding of the phosphotyrosine ligand (Schlessinger, 1994; Songyang *et al.*, 1993, 1994), and highly conserved in GIV (Figure 2b). Of note, the three X residues within this GXFXXR motif in GIV were unusual in that they were GDFYDR instead of the hydrophobic side chains that are typically seen in other SH2 proteins (Supplemental Figure S1). A phylogenetic analysis of GIV revealed that this motif is conserved in mammals, whereas it is absent in birds, fish, or lower animals (Figure 2c and Supplemental Figure S2). Therefore the GXFXXR motif of GIV, which is key to the functions of the SH2-like domain, is evolutionarily younger than the GEF motif (the latter evolves earliest in fish; Garcia-Marcos *et al.*, 2009) and the two critical C-terminal tyrosines that upon phosphorylation bind and activate PI3K (which evolved first in birds; Lin *et al.*, 2011; Supplemental Figure S2). Next we built a homology model of the putative SH2-like domain in the C-terminus of GIV using the ICM homology modeling procedure (Cardozo *et al.*, 1995, 2000; Abagyan *et al.*, 1997) and the available structures of SH2 domains and the GIV-SH2 sequence alignment (Supplemental Figure S1; see *Materials and Methods*). The modeled structure of human GIV-SH2 superimposed onto the known structure of SOCS3 (Protein Data Bank [PDB] 2hmh), another SH2 domain (Figure 2d), revealed that the putative SH2-like domain has the same characteristics as all other SH2 domains; they feature an antiparallel β-sheet flanked by α-helices and mostly short loops, and the α-helices and the edge of the β-sheet create a fairly flat surface for phosphopeptide binding. The homology model also provided clues into how the SH2-like domain remains stably folded in the presence of phosphotyrosine ligands despite its unusual polar composition. For example, both Asp-1741 and Asp-1744 within the ^{1740}GDFYDR^{1745} motif are buried compensated charges making multiple favorable polar interactions with the surrounding residue side chains in the folded state (Figure 2e). Specifically, the carboxyl group of Asp-1741 is in hydrogen-bonding proximity of hydroxyl groups of Tyr-1743 (also a part of ^{1740}GDFYDR^{1745}), Ser-1733, Ser-1828, and possibly the primary amine of Lys-1737. Similarly, Asp-1744 within the ^{1740}GDFYDR^{1745} motif is favorably close to the side chains of Ser-1714, Arg-1790, and Ser-1805. These findings indicate that the unusual polar residues found in the GXFXXR motif are stabilized in the folded (SH2-like) form and provide insights into the role of the unusual Tyr at 1743 within the ^{1740}GXFXXR^{1745} motif (Figure 2e).

A model of the complex between GIV's SH2-like domain and the EGFR-derived phosphotyrosine peptide containing pY1148 and its flanking sequence revealed that the phosphotyrosine binding pocket of GIV's SH2-like domain is mostly basic, which is compatible with binding to the acidic residues that flank Y1148 (and Y1173) of EGFR (Figure 2f). Because GIV's putative SH2-like domain shares weak

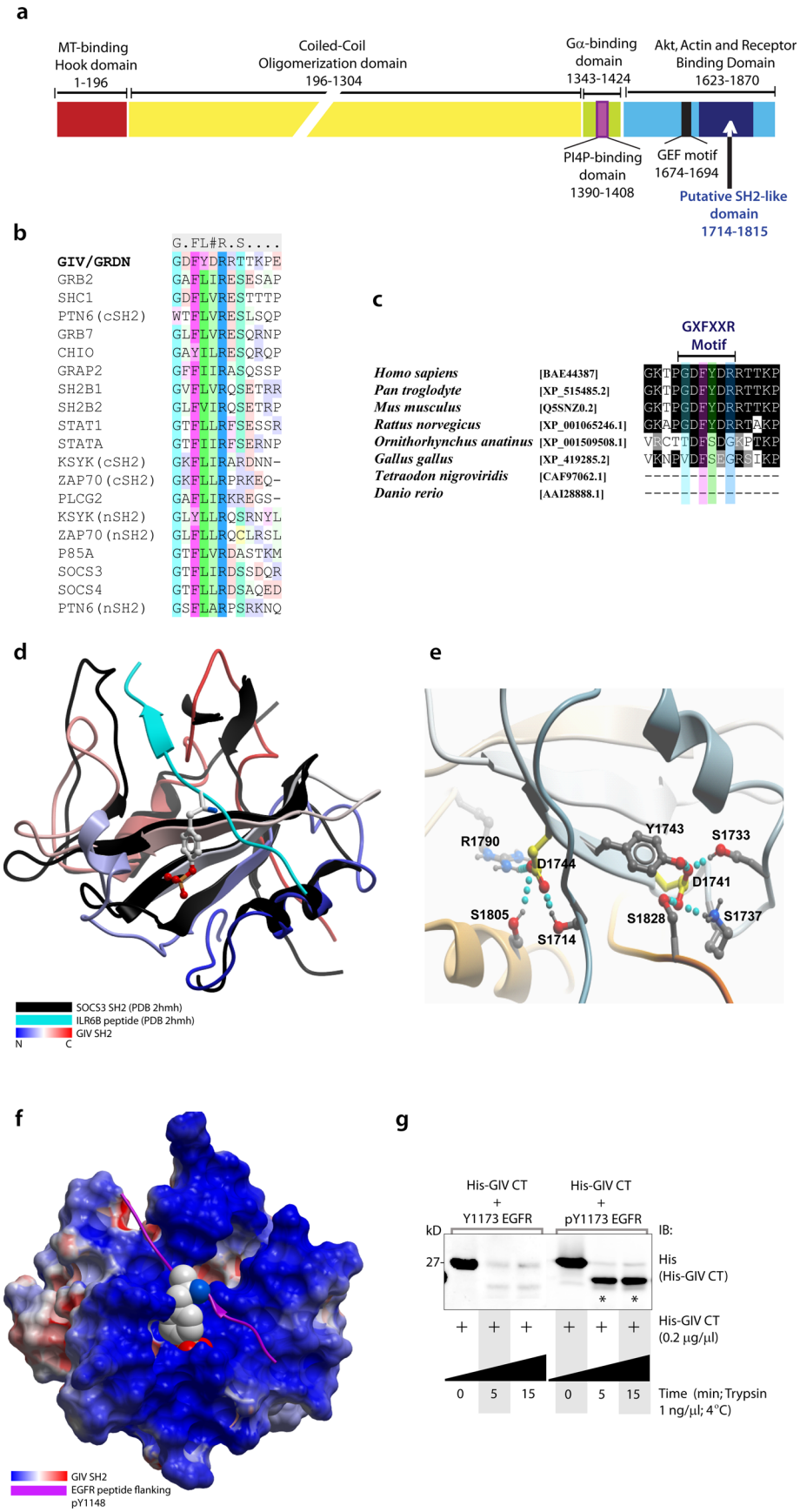

FIGURE 2: GIV's C-terminus folds into a SH2-like domain in the presence of phosphotyrosine ligand. (a) Schematic representation of the domain organization of GIV. The putative SH2-like domain (dark blue) is located in the C-terminus, ~15 aa downstream of the GEF motif (black), within the Akt and actin-binding domains (light blue). Other domains include a microtubule-binding hook domain (red), a coiled-coil homodimerization domain (yellow), a Gα-binding domain (GBD, green), and a PI4P-binding domain (purple). The numbers denote the amino acids marking the boundaries of each domain. (b) The sequence corresponding to the C-terminal domain of human (BAE44387, aa 1623–1870) GIV/Girdin was used to align with 19 other known SH2 domains in various proteins by pfam alignment using the MolSoft molecular modeling platform. Pfam contains multiple alignments and hidden Markov model–based profiles (HMM profiles) of complete protein domains. The GXFXXR motif that is conserved among all SH2-like domains and conserved in GIV is highlighted (see also Supplemental Figure S1). (c) The sequence corresponding to the C-terminal domain of human GIV (BAE44387, aa 1623–1870) was used to identify homologues by BLAST search. The phosphotyrosine recognizing GXFXXR motif of GIV is absent in fish, birds, and platypus (egg-laying mammals) but highly conserved in higher mammals (see also Supplemental Figure S2 for an extended alignment). (d) A structural model of GIV's C-terminal sequence (aa 1714–1815; depicted as a ribbon, colored blue to red from N- to C-terminus) was built based on the alignment with 43 known SH2 templates using ICM software (MolSoft). Superimposition of the model onto an established SH2 domain complex structure (C-terminal SH2 domain of SOCS3 [black] bound to LR63 phosphopeptide derived [teal blue], PDB 2hmh) illustrates fold similarity. (e) Predicted atomic environment of the polar residues in the 1740-GDFYDR-1745 motif in the GIV CT in its folded SH2-like state. Asp1741, Tyr1743, and Asp1745 are shown in yellow. These residues are polar, unlike the corresponding residues in typical SH2 domains. In the predicted folded SH2 state, residues in gray make favorable polar interactions (cyan) with the residues in yellow. (f) Molecular modeling of the interface between GIV's SH2 domain and EGFR-derived phosphotyrosine peptide (purple) corresponding to pTyr1148 and its flanking residues, a high-affinity binding site for GIV on the EGF receptor. The acidic, neutral, and basic potentials are displayed in red, white, and blue, respectively. The electrostatic surface potential of the phosphotyrosine-recognizing and -binding pocket of GIV's SH2 domain is mostly basic. (g) Equal aliquots of His-GIV CT were first incubated with 10-fold molar excess of commercially synthesized pY1173EGFR or dephosphorylated control EGFR peptides before subjecting it to limited tryptic proteolysis on ice. Reactions were analyzed for GIV-CT (His) by IB. A trypsin-resistant product of ~15 kDa is seen (asterisk) exclusively when His-GIV-CT is preincubated with phosphorylated EGFR peptide. Using His-GIV-CT-RL as substrate, it was confirmed that addition of pY1173EGFR peptide alone did not inhibit trypsin's protease activity (unpublished data).

sequence similarity with other SH2 proteins with an unusually polar composition and multiple strategies for expression and purification of GIV's ~110-aa-long SH2-like domain from bacteria failed, we asked whether GIV's SH2-like domain represents a transient state that folds only in the presence of ligand (phosphotyrosines on RTK tail) but remains unstructured or poorly structured in physiology. We explored this possibility using limited proteolysis, a simple biochemical method that can reveal large changes in protein conformation. When we incubated purified histidine (His)-GIV-CT with phosphorylated or dephosphorylated Y1173EGFR peptides and subsequently carried out limited proteolysis with trypsin, we found that His-GIV-CT was highly susceptible to proteolysis when preincubated with dephosphorylated Y1173EGFR peptide but relatively resistant to proteolysis when preincubated with phosphorylated Y1173EGFR peptide, a natural ligand for GIV's SH2-like domain (Figure 2g). These results are consistent with the possibility that GIV's C-terminus folds into trypsin-resistant conformation exclusively in the presence of pY ligand. These findings, together with the fact that most sequence analysis programs predicted this region to be poorly structured, likely due to the unusual abundance of polar residues, suggest that this region of GIV-CT may have properties of structural plasticity between an intrinsically disordered state during quiescence and a folded SH2-like modular state when engaged with multiple RTKs.

GIV's SH2-like domain is required and sufficient to recognize and bind ligand-activated RTKs

To determine whether GIV-CT folds into a SH2-like module and recognizes/binds to phosphotyrosine ligands, as predicted by the homology model in Figure 2, we made a number of predictions by computational modeling regarding the effect of strategically placed mutations within GIV's SH2-like domain (Figure 3, a and b): 1) mutations in the core GXFXXR motif and phosphotyrosine binding pocket that were predicted to abolish the GIV:EGFR interaction, 2) mutations within adjacent sequences that do not participate in phosphotyrosine recognition and were predicted to be inconsequential, and 3) a mutation within the pocket that was expected to favor binding. We found all these predictions to be accurate when we carried out binding assays using various His-tagged GIV mutants and in vitro–phosphorylated, GST-tagged pY1148 EGFR tail peptide (Figure 3, c and d); that is, compared with GIV–wild type (WT), some mutants abolished binding (lanes 2, 4–6, and 8), whereas others bound equally well (lanes 3, 9, and 10) or consistently better (F1765T; ~1.45-fold, $p < 0.01$). These findings validate our homology model of GIV-SH2 (Figure 2, d and f) and demonstrate that the conserved *GXFXXR*' core motif and the flanking sequence that the C-terminus of GIV shares with other SH2 adaptors can function as a SH2-like domain, in that they recognize and directly bind phosphotyrosine ligands. These results also indicate that the ~100- to 110-aa stretch within GIV's C-terminus is likely to assume a SH2-like domain structure as predicted by homology modeling (Figure 2).

Next we asked whether the isolated SH2-like domain is sufficient for GIV to bind EGFR in cells. We used a bimolecular fluorescence complementation (BiFC) approach, in which interaction between two proteins, each tagged with the N- or C-terminus of Venus–yellow fluorescent protein (YFP; VN or VC), is assessed by the abundance and distribution of fluorescence emitted by a functionally folded Venus-YFP protein only when the two proteins are within 10 nm of each other for a significant duration of time (Shyu *et al.*, 2008). We found that cells coexpressing EGFR-VC and a WT VN-GIV-SH2-like domain (aa 1714–1815; Figure 3. e and f) display yellow fluorescence at the plasma membrane (PM) and on vesicular structures, presumably endosomes (Figure 3f). No such fluorescence was detected when the critical Arg within the *GXFXXR*' motif, which was indispensable for GIV to recognize and bind phosphotyrosines on the EGFR tail (Figure 3d), was mutated to Leu (R1745L; henceforth referred to as RL). Taken together, these results demonstrate that a functional SH2-like domain at its C-terminus is required and sufficient for GIV to recognize and directly bind sites of autophosphorylation on the EGFR tail.

GIV's GEF and SH2-like domains cooperatively recruit Gαi to ligand-activated RTKs and trigger its subsequent activation

Next we investigated the functional relationship between GIV's SH2-like domain and its previously defined GEF motif (Garcia-Marcos *et al.*, 2009), which binds and activates Gαi. To determine whether an intact GEF motif is required for GIV's SH2 domain to bind phosphotyrosines, we used His-GIV-CT WT or mutant proteins that are either GEF-deficient (FA) or SH2-deficient (RL) in binding assays with in vitro–phosphorylated, GST-tagged pY1148 EGFR tail. We found that the WT GIV-CT and the FA mutant bound phosphorylated EGFR tail to an equal extent, whereas the RL mutant did not (Figure 4a), indicating that in the absence of an intact GEF motif, GIV's SH2-like domain is sufficient to recognize and bind phosphotyrosines on the EGFR tail. To whether if an intact SH2-like domain is required for GIV's GEF motif to bind and activate Gαi, we used the His-GIV-CT proteins in binding assays with GDP-loaded GST-Gαi3 (Figure 4b) and in steady-state GTPase assays with His-Gαi3 (Figure 4c). We found that the WT GIV-CT and the RL mutant bound (Figure 4b) and activated (Figure 4c) Gαi3 to an equal extent, whereas the FA mutant did not, demonstrating that the SH2-like domain is not required for GIV to bind and activate Gαi3. To determine the contribution of GIV's SH2-like domain and its GEF motif in the formation of Gαi-GIV-EGFR ternary complexes, we carried out binding assays with three recombinant proteins—His-Gαi3, His-GIV-CT, and in vitro–phosphorylated GST-pY1148 EGFR tail. We found that Gαi3 bound phosphorylated EGFR tail exclusively in the presence of WT GIV-CT (Figure 4d), indicating that the Gαi3-EGFR interaction is indirect and requires GIV-CT. This interaction was abolished when the WT GIV-CT protein was replaced by either the SH2-deficient or the GEF-deficient mutant (Figure 4d), indicating that both the SH2-like domain and the GEF motif are required for GIV to facilitate the interaction between Gαi3 and EGFR and to trigger the assembly of Gαi3-GIV-EGFR ternary complexes in vitro.

Next we asked whether GIV's SH2-like domain is required for the recruitment of Gαi3 to ligand-activated EGFR. To this end, we analyzed receptor-bound immune complexes (Figure 4e) before and after ligand stimulation in GIV-depleted HeLa cells stably expressing small interfering RNA (siRNA)–resistant, FLAG-tagged WT and mutant GIV (Supplemental Figure S3, A and B). As shown previously (Ghosh *et al.*, 2010), Gαi3 coimmunoprecipitated with EGFR exclusively after ligand stimulation in HeLa GIV-WT cells but not in HeLa GIV-FA cells, which express GEF-deficient GIV mutant (Figure 4e). Gαi3 was also undetectable in EGFR-bound complexes immunoprecipitated from HeLa GIV-RL cells, which express SH2-deficient GIV mutant, indicating that recruitment of Gαi3 to ligand-activated EGFR requires both the SH2-like domain and GEF motif in GIV to remain intact. We found that recruitment of Gαi3 to other RTKs—for example, ligand-activated InsR—also requires an intact SH2-like domain in GIV, because Gαi3 coimmunoprecipitated with InsR exclusively after ligand stimulation in HeLa GIV-WT but not in HeLa GIV-RL cells (Supplemental Figure S4).

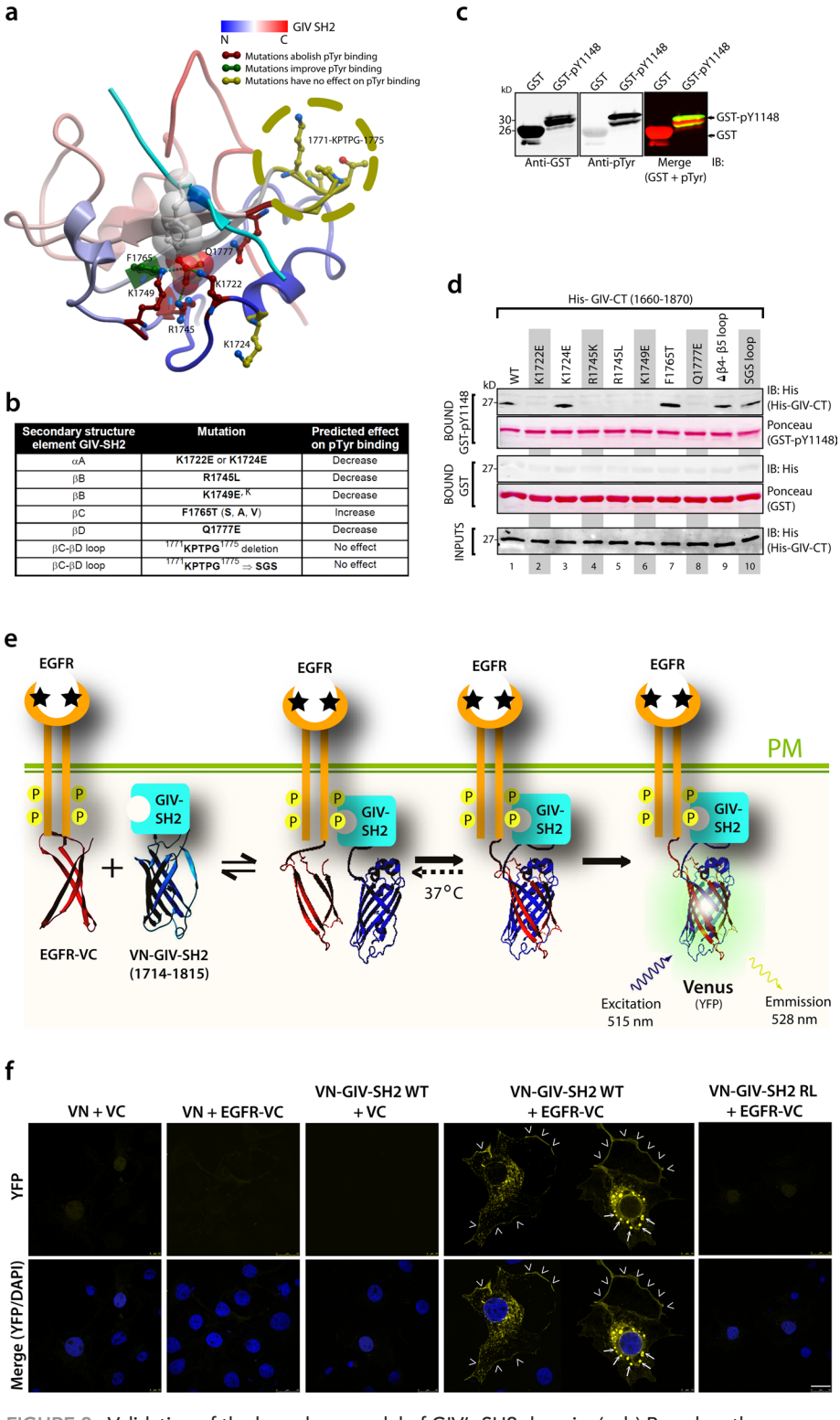

Secondary structure element GIV-SH2	Mutation	Predicted effect on pTyr binding
αA	**K1722E** or **K1724E**	Decrease
βB	**R1745L**	Decrease
βB	**K1749E**, K	Decrease
βC	**F1765T** (S, A, V)	Increase
βD	**Q1777E**	Decrease
βC-βD loop	^{1771}**KPTPG**^{1775} deletion	No effect
βC-βD loop	^{1771}**KPTPG**^{1775} ⇒ **SGS**	No effect

FIGURE 3: Validation of the homology model of GIV's SH2 domain. (a, b) Based on the generated three-dimensional model shown in Figure 2, d and e, a series of GIV C-terminal mutations were predicted to decrease, increase, or have no effect on the recognition and binding to the phosphotyrosine 1148 on the cytoplasmic tail of EGFR. These residues are highlighted in red, green, and gold, and listed along with the preferred amino acid substitution in b. R1745 of GIV corresponds to the invariant Arg residue at the βB5 position within the conserved *GXFXXR* motif that is characteristic of the entire SH2 family of adaptors (Songyang *et al.*, 1993, 1994; Schlessinger, 1994). The βC-βD loop, which is predicted to not affect phosphotyrosine binding, was either deleted or replaced with a neutral flexible linker, SGS. F1765 was mutated to Thr (T) to resemble the mouse sequence; this substitution is predicted to increase the depth of the binding pocket and improve binding. α, helix; β, β-sheets.

Next we asked whether GIV-dependent recruitment of Gαi to ligand-activated RTKs affects G protein activation downstream of ligand-activated receptors. When we carried out immunoprecipitation assays with an antibody that has been characterized extensively (lane *et al.*, 2008) and specifically recognizes the active conformation of GTP-bound Gαi (Supplemental Figure S5), we found that Gαi was activated in HeLa-GIV WT exclusively after EGF stimulation but not in HeLa GIV-RL, indicating that GIV's SH2 domain is required for Gαi activation downstream of EGFR (Figure 4f). Consistent with differential activation of Gαi in the two cell lines, cellular cyclical AMP (cAMP), a second messenger produced by adenylyl cyclase, was elevated (Figure 4g), and phosphorylation of cAMP response element–binding protein (CREB) was enhanced in GIV-RL cells compared with GIV-WT cells (Figure 4h). Taken together, these findings demonstrate 1) that the two functional modules of GIV, the SH2-like domain and the GEF motif, function independent of each other in the context of receptor recognition and enzyme (GEF) activity, respectively, but 2) they cooperate to form the RTK-GIV-Gαi ternary complexes (in vitro and in cells) and activate Gαi downstream of growth factor receptors.

(c, d) Equal aliquots (25 µg) of GST and GST-pY1148 were phosphorylated in vitro using recombinant EGFR kinase and used in pull-down assays with purified WT or various mutants of His-GIV-CT listed in b. (c) An aliquot of the GST proteins was analyzed for GST and pTyr by IB. Yellow pixels in the overlay images (merge panels) confirm that GST-pY1148 is autophosphorylated on tyrosine(s) by EGFR kinase in vitro. (d) Bound GIV CT was visualized by IB for His. Equal loading of GST and GST-pY1148 was confirmed by Ponceau S staining. A representative experiment is shown; $n = 4$. (e) Schematic representation of EGFR-VC and VN-GIV-SH2 constructs used for BiFC assay. (f) Cos7 cells were cotransfected with indicated complementary pairs of probes, grown in 10% FBS, fixed, and analyzed for fluorescence by confocal microscopy. Images representative of each condition are shown. Fluorescence is observed at the PM (arrowheads) and on vesicles (arrows; likely endolysosomal compartments) exclusively when complementary VN-GIV-SH2 WT, but not the SH2-deficient RL mutant probe, was cotransfected with EGFR-VC. Paired transfection of other complementary VN- and VC-control probes did not show discernible fluorescence (~400 cells/experiment; $n = 4$).

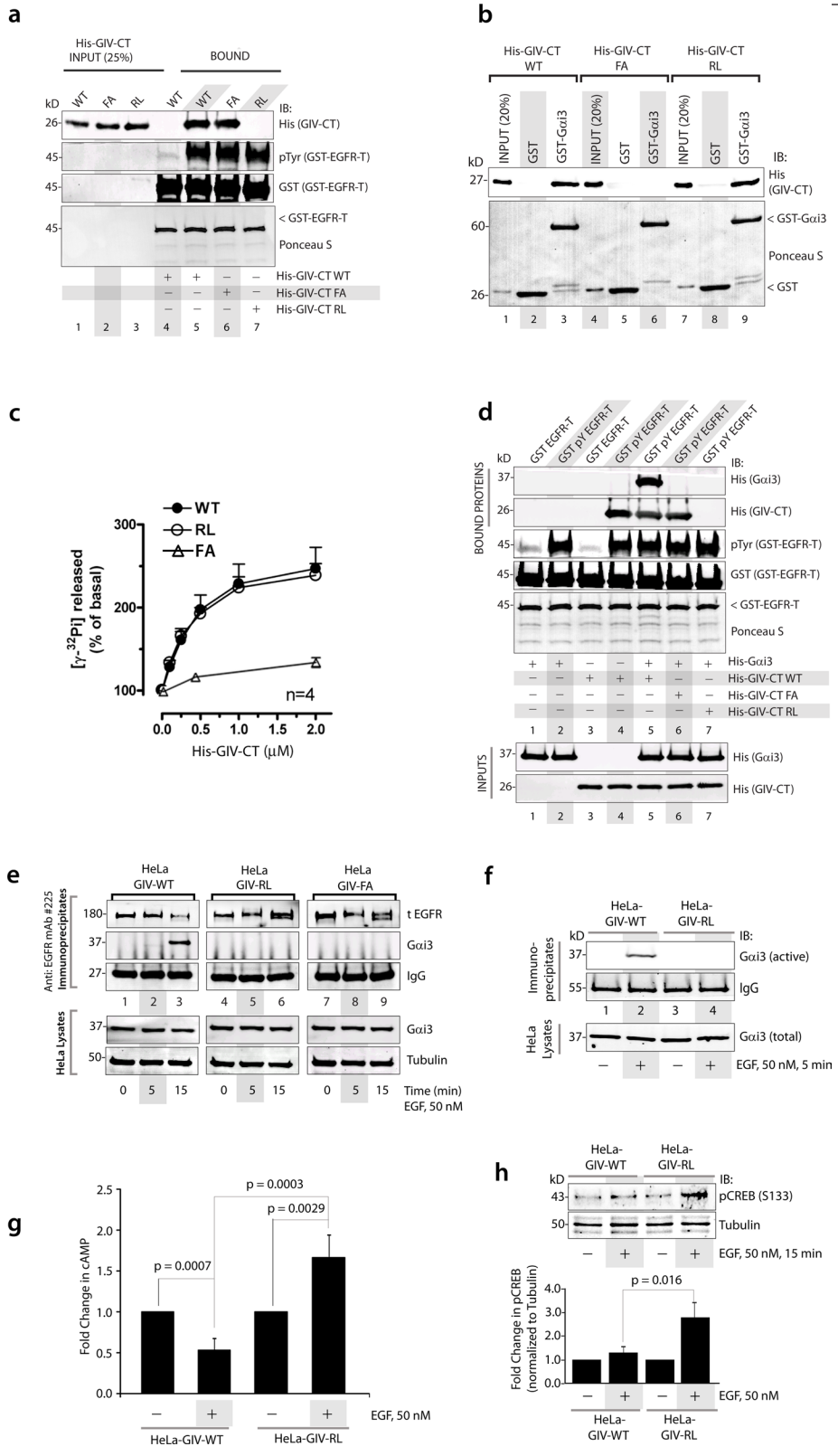

FIGURE 4: GIV's SH2 and GEF domains are required for the recruitment of Gαi3 to ligand-activated EGFR and activation of G protein after EGF stimulation. (a) Equal aliquots (15 μg) of GST-EGFR-T (aa 1064–1210) were either phosphorylated in vitro using 5 ng of recombinant EGFR kinase (GST-pY EGFR-T; lanes 5–7) or mock treated (GST-EGFR-T; lane 4) and subsequently used in pull-down assays with equal amounts of purified WT, FA (GEF-deficient), or RL (SH2-deficient) mutants of His-GIV-CT (aa 1660–1870; lanes 1–3, inputs). Bound proteins were analyzed for His-GIV-CT and phosphorylation of GST-EGFR-T by IB. As anticipated, GST-pY EGFR-T (lane 5) but not GST-EGFR-T (lane 4) directly binds His-GIV-CT WT. The FA (lane 6) but not RL (lane 7) mutant of GIV-CT binds GST-pY EGFR-T. (b) WT, FA, and RL mutants of His-GIV-CT were incubated with 5 μg of GST-Gαi3 or GST preloaded with GDP immobilized on glutathione beads. Bound proteins were analyzed by IB for GIV-CT using anti-His mAb. His-GIV-CT WT (lane 3) and RL mutant (lane 9) bound GST-Gαi3 equally, and, as anticipated, the FA mutant did not (lane 6). (c) The amount of GTP hydrolyzed in 10 min by His-Gαi3 was determined in the presence of the indicated amounts of WT (Δ), FA (Δ), and RL mutant (•) His-GIV-CT. Both WT and RL mutants increased the steady-state GTPase activity of His-Gαi3 efficiently and equally in a dose-dependent manner, whereas the FA mutant did not. The basal steady-state GTPase activity of His-Gαi3 is 0.021 ± 0.04 mol Pi mol $Gαi3^{-1}$ min^{-1} and the results are displayed as percentage of basal activity. (d) Equal aliquots (15 μg) of GST-EGFR-T (aa 1064–1210) were either phosphorylated in vitro with recombinant EGFR kinase (GST-pY EGFR-T; lanes 2 and 4–7) or mock treated (GST-EGFR-T; lanes 1 and 3) and subsequently used in pull-down assays with purified His-Gαi3 alone (lanes 1 and 2), His-GIV-CT alone (lanes 3 and 4), or a mix of His-Gαi3 and WT, FA, or RL mutants of His-GIV-CT as indicated. Bound proteins were analyzed for His-GIV-CT and phosphorylation of GST-EGFR-T by IB. Gαi3 binds GST-pY EGFR in the presence of WT (lane 5) but not FA (lane 6) or RL (lane 7). (e) HeLa GIV-WT, HeLa GIV-FA, and HeLa GIV-RL cells stably expressing the indicated siRNA-resistant GIV constructs were depleted of endogenous GIV by siRNA, serum starved for 16 h, and then stimulated with EGF for the indicated durations before lysis. Equal aliquots of lysates (bottom) were incubated with anti-EGFR mAb (#225 IgG). Immune complexes (top) were analyzed for total (t-EGFR) and Gαi3 by IB. (f) Equal aliquots of lysates (bottom) from starved or EGF-treated HeLa GIV-WT and GIV-RL cells were incubated with anti-Gαi:GTP mAb. Immune complexes (top) were analyzed for Gαi3 by IB. (g) HeLa-GIV-WT and GIV-RL cells were depleted of endogenous GIV as in e, serum starved (0.2% FBS), and subsequently stimulated with EGF and analyzed for cAMP by RIA (see *Materials and Methods*). Results are displayed as fold change in cAMP (*y*-axis) in each cell line normalized to their respective starved state. (h) HeLa-GIV-WT and GIV-RL cells were stimulated with EGF before lysis as in e. Top, equal aliquots of whole-cell lysates were analyzed for phosphorylated CREB (pCREB) and tubulin by IB. Bottom, bar graphs display the quantification of pCREB/tubulin by band densitometry. All values are normalized to the starved HeLa-GIV-WT cells. Results are shown as mean ± SEM; $n = 3$.

GIV-SH2 domain is required for tyrosine phosphorylation of GIV by RTKs

We previously demonstrated that upon ligand stimulation, multiple RTKs phosphorylate GIV at two critical tyrosines, Y1764 and Y1798, and that both sites are capable of binding and activating class 1A PI3Ks (Lin *et al.*, 2011). Although these two tyrosines are located within the boundaries of the SH2-like domain of GIV (Figure 5a and Supplemental Figure S6a), the homology model predicts that they are exposed and accessible to RTKs (Figure 5a). We asked whether receptor-mediated phosphorylation of GIV in cells requires an intact SH2-like domain of GIV, thereby bringing the substrate (GIV) in proximity to the kinase (EGFR). To answer this, we compared the extent of EGF-stimulated tyrosine phosphorylation of wild-type GIV to the SH2-deficient RL mutant and a previously described phosphorylation-deficient GIV-YF mutant (Lin *et al.*, 2011); the latter is a negative control in which both tyrosines were replaced by Phe (F). Because nonreceptor TKs of the Src family can also phosphorylate GIV on those two tyrosines (Lin *et al.*, 2011), we used the kinase inhibitor PP2 to abolish any contribution to GIV phosphorylation via the Src family of kinases, exactly as we used previously (Lin *et al.*, 2011; Mittal *et al.*, 2011). On EGF stimulation, wild-type GIV, but not the RL and the YF mutants, was tyrosine phosphorylated (Figure 5b), indicating that an intact SH2-like domain is essential for enhanced tyrosine phosphorylation in GIV. Because EGFR kinase phosphorylated the RL mutant just as efficiently as WT GIV-CT in vitro (Supplemental Figure S6b), its failure to be phosphorylated in cells (Figure 5b) indicates that the SH2-like function of GIV is required for enhanced phosphorylation of GIV by EGFR in cells.

Because protein phosphorylation predominantly occurs within intrinsically disordered regions of substrate proteins (Iakoucheva *et al.*, 2004) and the two tyrosines of GIV are abundantly phosphorylated despite being located within a SH2-like folded region, we asked whether RTKs phosphorylate GIV when it is intrinsically disordered before folding into a SH2-like domain. We found that this is indeed the case, because recombinant EGFR failed to phosphorylate His-GIV-CT when it was preincubated with its pY1173EGFR ligand (bound/folded in a trypsin-resistant conformation as in Figure 2h) but robustly phosphorylated it when incubated with the dephosphorylated control peptide (Figure 5c). These results indicate that phosphorylation of GIV-CT must proceed before it completes folding into a stable SH2-like domain. We also found that both ligand-stimulated EGFR (Figure 5d) and InsR (Figure 5e) coimmunoprecipitate with pY1764GIV, indicating that tyrosine phosphorylated GIV's SH2-like domain is capable of stably binding RTKs. Taken together, these results indicate that the dynamic interplay of RTKs with GIV is comprises two events that closely follow each other: 1) recognition of autophosphorylated RTK tail by GIV-CT via a SH2-like mechanism is essential for RTKs to efficiently phosphorylate GIV, and such phosphorylation occurs when GIV-CT is still in a partially disordered state; and 2) completion of folding of phosphorylated GIV-CT into a SH2-like module, which allows tyrosine-phosphorylated GIV to be stably recruited to ligand-activated RTKs.

GIV-SH2 modulates EGFR signaling by regulating adaptor recruitment to activated receptor

We previously demonstrated (Ghosh *et al.*, 2010) that GIV enhances receptor autophosphorylation, affects the recruitment of key signaling adaptors to the receptor tail, and alters several major EGF signaling pathways such that they are either selectively amplified (e.g., PI3K/Akt) or attenuated (e.g., mitogen-activated protein kinase/extracellular signal-regulated kinase [MAPK/ERK]) via poorly understood mechanisms. We reasoned that by virtue of its ability to directly bind pY1148 and 1173 on EGFR tail, the newly identified SH2-like domain in GIV may shape EGF signaling by affecting the profile of SH2 adaptor recruitment to the ligand-activated receptor tail. We focused on Shc1 and SHP1, two SH2 adaptors that are major players in shaping EGF signaling (Keilhack *et al.*, 1998; Sakaguchi *et al.*, 1998), because they bind EGFR predominantly at the sequences flanking pY1148 and pY1173: Shc1 binds primarily to pY1148 and weakly to pY1173 (Okabayashi *et al.*, 1994), whereas SHP1 binds primarily to pY1173 and weakly to pY1148 (Keilhack *et al.*, 1998). In GST pull-down assays with immobilized phosphorylated GST-EGFR tail pY1173 peptide, increasing amounts of His-SHP-1, and constant amounts of His-tagged GIV-CT proteins in solution, we found that increased binding of SHP1 coincided with decreased binding of GIV-CT to EGFR phosphopeptide (Figure 6a), indicating that SHP1 and GIV-CT compete for pY1173 on EGFR tail. Similarly, in GST pull-down assays with immobilized phosphorylated GST-EGFR tail pY1148 peptide, increasing amounts of His-tagged GIV-CT, and constant amounts of Shc1 proteins in solution, we found that increased binding of GIV coincided with decreased binding of Shc1 to EGFR phosphopeptide (Figure 6b), indicating that Shc1 and GIV-CT compete for pY1148 on EGFR tail. To determine whether such competition occurs in cells, we evaluated the profile of SH2-adaptor recruitment to the EGFR tail in GIV-WT versus GIV-RL HeLa cells by immunoprecipitating the receptor and analyzing the receptor-bound complexes by immunoblotting (IB). We found that the profile of adaptor recruitment was significantly different in the two cell lines. GIV was recruited to ligand-activated EGFR in GIV-WT but not in GIV-RL cells (Figure 6c). When GIV failed to be recruited to EGFR in GIV-RL cells, recruitment of p85α (PI3K) and Grb2 was also suppressed but recruitment of SHP1 and Shc1 was enhanced. Consistent with the enhanced recruitment of SHP1, in GIV-RL cells, we observe that activation of SHP1, as determined by the abundance of pY536SHP1 (Figure 6c, Lysates), and dephosphorylation of key autophosphorylation sites in EGFR (Figure 6c, Immunoprecipitates) were enhanced. Together these results demonstrate that binding of GIV-SH2 competes with SHP1 and Shc1 for binding to two major sites of autophosphorylation on EGFR.

We also found that presence or absence of an intact SH2 domain in GIV is a key determinant of how two major downstream pathways are modulated (Figure 6d): in GIV-RL cells, activation of the PI3K/Akt pathway, as determined by Akt phosphorylation, was suppressed, whereas activation of the MAPK/ERK pathway, as determined by ERK phosphorylation, was enhanced compared with GIV-WT cells. Together these results demonstrate that the GIV-SH2 domain affects the earliest events in EGF signaling—SH2-adaptor recruitment and the pattern of receptor autophosphorylation—by competing with key adaptors that shape major downstream signaling pathways.

On the basis of our results so far, we propose the following model (Figure 6e). In cells with little or no GIV expression or in those expressing GIV mutants/isoforms lacking the C-terminus or a functional SH2-like domain, ligand-activated EGFR triggers unopposed recruitment of Shc1 and SHP-1 adaptors, which in turn ensures enhancement of the MAPK/ERK pathway by Shc1 and rapid receptor dephosphorylation by SHP-1. In cells expressing high copies of functionally intact GIV, GIV-SH2 competes with both Shc1 and SHP-1 for binding sites on EGFR tail. Recruitment of GIV's SH2-like domain to EGFR suppresses/terminates Shc1-mediated MAPK/ERK activation and antagonizes SHP-1–mediated receptor dephosphorylation while simultaneously triggering two other pathways in parallel—1) GIV's GEF function links G protein activation to ligand-activated receptor, and 2) EGFR phosphorylates GIV on tyrosines that help

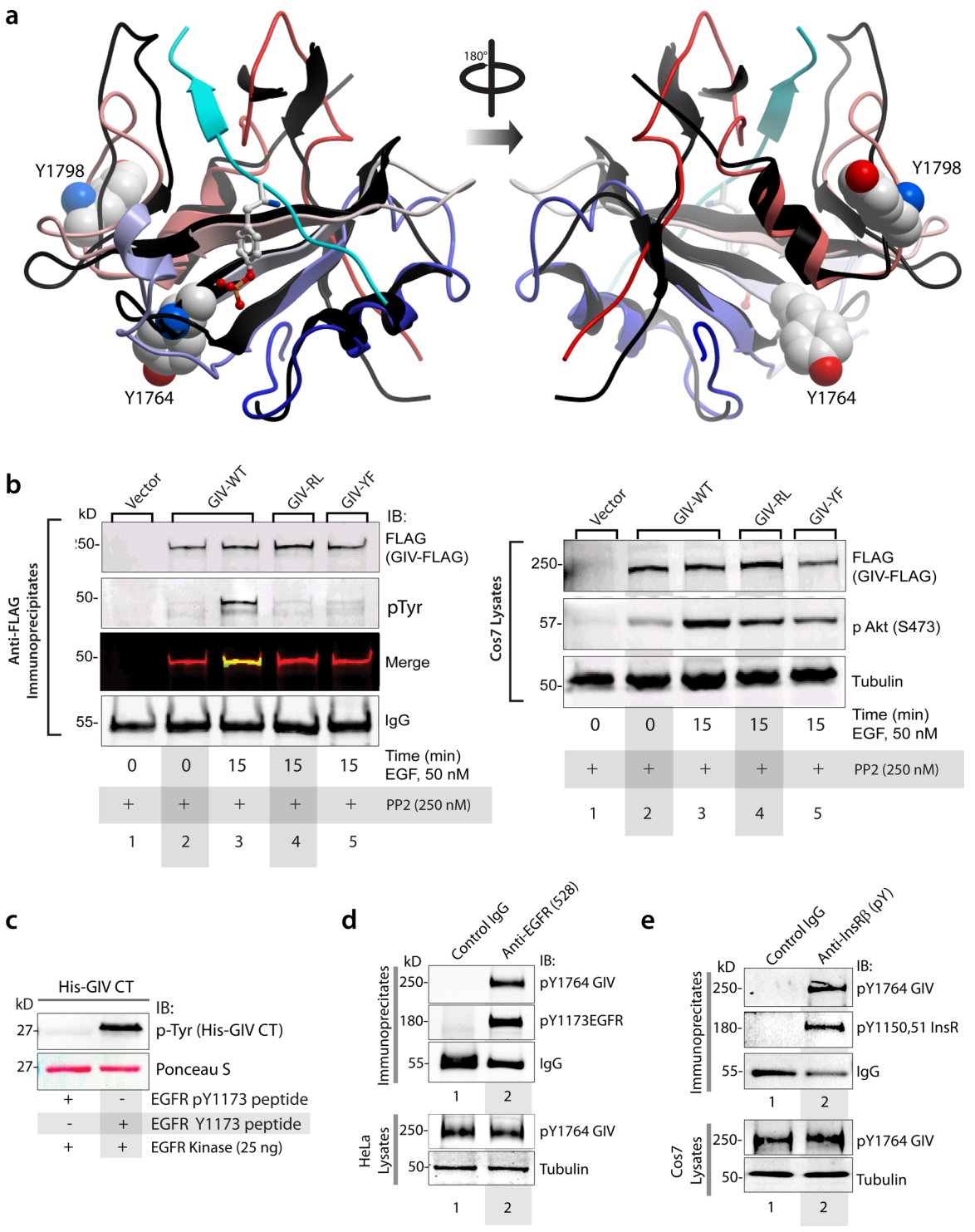

FIGURE 5: The SH2-like domain of GIV is required for enhanced tyrosine phosphorylation of GIV and subsequent binding to RTKs. (a) Homology model of GIV's SH2 domain is depicted as a ribbon as in Figure 2d. The positions and the orientations of the two tyrosines are displayed in two views: from the "front" (pTyr-binding interface) and "back." Both tyrosines are well exposed to solvent, consistent with the fact that multiple receptor and nonreceptor tyrosine kinases can readily access and phosphorylate them and that they can directly bind and activate PI3K (Lin *et al.*, 2011). (b) Cos7 cells expressing FLAG-tagged wild-type GIV (GIV-WT FLAG), SH2-deficient R1745L mutant GIV (GIV-RL FLAG), a tyrosine phosphorylation–deficient mutant (GIV-YF FLAG; Lin *et al.*, 2011), or vector alone were serum starved, pretreated with Src inhibitor (PP2), and subsequently stimulated with EGF before lysis. GIV was immunoprecipitated from equal aliquots of lysates (right) with FLAG mAb, and immunoprecipitates (left) were analyzed for GIV (red) and pTyr (green) by IB and dual-color imaging. The merge confirms that tyrosine-phosphorylated GIV (yellow) was immunoprecipitated exclusively from EGF-treated cells expressing GIV-WT (lane 3) but not from cells expressing GIV-RL (lane 4). As shown previously (Lin *et al.*, 2011), the negative control GIV-YF was not phosphorylated (lane 5). The lysates (right) were analyzed for FLAG (GIV-FLAG), phospho-Akt (pAkt), and tubulin by IB. (c) Equal aliquots of His-GIV-CT

recruit and activate PI3K, thereby triggering the activation of Akt kinase.

GIV-SH2 regulates EGFR trafficking, degradation, actin remodeling, and cell migration

We previously demonstrated (Ghosh *et al.*, 2010) that GIV induces rapid degradation of EGFR after receptor endocytosis, thereby reducing the duration of signaling from endosomes. Because the SH2-like domain of GIV alters key early events in EGF signaling, we reasoned that it might also be responsible for altering the rate of receptor degradation. When we investigated this in HeLa-GIV-WT, -FA, and -RL cells by immunofluorescence (Figure 7a) and immunoblotting (Figure 7b), both approaches showed that rates of receptor degradation were faster in GIV-WT cells but slower in GIV-RL cells, with significant amounts of receptor lingering at 30 and 60 min (Figure 7, a and b) within EEA1-positive endocytic compartments (Figure 7a). Consistent with our prior work, the rate of receptor degradation was delayed also in GIV-FA cells. Because both GIV-RL and GIV-FA are deficient in assembling ternary RTK-GIV-Gαi complexes, these results indicate that both SH2 and GEF domains, which cooperatively assemble such ternary complexes (Figure 4), are required for efficient down-regulation of activated receptor in endocytic compartments.

Finally, we asked whether the two previously identified major downstream phenotypes attributed to GIV (Enomoto *et al.*, 2005; Ghosh *et al.*, 2011)—actin remodeling and cell migration—were affected in the absence of an intact SH2-like domain in GIV. We found that indeed such was the case, because GIV-RL cells, in which GIV is functionally uncoupled from ligand-activated EGFR, formation of actin stress fibers, and efficient two-dimensional cell migration in scratch-wound assays, were impaired (Figure 7, d and e). Taken together, these results demonstrate that the SH2-like domain described here is a critical domain that links RTKs like EGFR to signal transduction and modulation of cellular phenotype via GIV.

DISCUSSION

GIV is a unique SH2-like adaptor and imparts GEF activity for trimeric G proteins to RTKs

The major finding in this work is the discovery that GIV, a previously described nonreceptor GEF for Gαi, is a novel SH2-like adaptor that links multiple ligand activated RTKs—for example, EGFR and InsR to activation of trimeric Gi proteins. We previously demonstrated that the GEF domain of GIV is required for assembly of GIV:Gαi signaling interface, which activates Gαi (Garcia-Marcos *et al.*, 2009). Here we show that adjacent to the GEF motif is a stretch of ~110 aa within GIV's C-terminus that recognizes autophosphorylated tyrosines on cytoplasmic tails of ligand-activated RTKs and stably folds into a SH2-like module to assemble the RTK:GIV signaling interface. It is this coexistence of G protein–activating GEF and RTK-binding SH2 modules in tandem within GIV's C-terminus that allows for convergence of two pathways on a common GIV platform. We provide evidence demonstrating how these two domains cooperatively assemble RTK (activated)-GIV-Gαi ternary complexes in vitro and in cells. When GIV is uncoupled from EGFR (i.e., in cells expressing SH2-deficient GIV mutants), both recruitment of Gαi to the ligand-activated receptor and subsequent activation of the G protein in response to EGF are abolished. Therefore our discovery of a SH2-like domain in GIV explains how RTKs trigger activation of Gi proteins and sheds light on the long-standing questions surrounding RTK/G protein cross-talk.

The significance of our findings also lies in the fact that none of the other >100 SH2 adaptors that were identified before GIV (Liu *et al.* 2011) possesses intrinsic GEF activity toward trimeric G proteins or, for that matter, ability to either bind or modulate any other aspect of trimeric G protein signaling. Similarly, GIV is a rare example within a growing family of nonreceptor modulators of G proteins (GEFs, GTPase-activating proteins, and GDP dissociation inhibitors; Siderovski and Willard, 2005) with a structural module that recognizes and binds ligand-activated RTKs. Moreover, the discovery of a SH2-like domain within GIV's C-terminus as the structural basis for how GIV binds ligand-activated, autophosphorylated RTKs provides mechanistic insights into our observation that GIV activates Gαi downstream of multiple growth factors during a variety of cellular processes (Garcia-Marcos *et al.*, 2009, 2011a; Ghosh *et al.*, 2010; Lopez-Sanchez *et al.*, 2014; Wang *et al.*, 2014). We conclude that the unique combination of GEF and SH2 domains in GIV constitutes a novel platform for cross-talk that relays signals from ligand-activated growth factor RTKs to Gi proteins.

Furthermore, we demonstrate that GIV's C-terminal ~100-aa stretch that folds into a SH2-like domain is intrinsically disordered or partially structured in the resting state. Folding into a trypsin-resistant stable structure occurs when autophosphorylated tyrosines on cytoplasmic tails of RTKs are available, which are the natural ligand for GIV's SH2-like domain. In that way, GIV joins the rank of numerous examples of eukaryotic proteins that are intrinsically disordered or partially structured under physiological conditions and fold into functional modules, especially in the context of signal transduction (Iakoucheva *et al.*, 2002; Dyson and Wright, 2002, 2005; Dunker *et al.*, 2008). Such proteins, while structurally poor, are functionally rich by virtue of the flexibility of their modular structures. We conclude that much like those intrinsically disordered proteins, GIV's SH2-like folded structure is induced upon binding to its biological target, that is, activated RTKs. Evolution of such structural plasticity in GIV is likely to assemble distinct interactomes in the disordered versus SH2-folded states, thereby contributing to functional enrichment. Because GIV's C-terminus is enriched in Ser/Thr residues, some of which are heavily phosphorylated (www.phosphosite.org), it is possible that additional phosphoevents on GIV's C-terminus trigger and/or regulate folding of GIV's SH2-like domain and binding to RTKs.

proteins were first incubated with 10-fold molar excess of either phosphorylated (left lane) or unphosphorylated (right lane) EGFR tail peptides (sequence flanking Y1173) before in vitro kinase assays with recombinant EGFR kinase. GIV-CT is phosphorylated only in the presence of dephosphorylated EGFR peptide (which it cannot bind) but not in the presence of phospho-EGFR ligand. (d) EGFR was immunoprecipitated from lysates of HeLa cells starved and stimulated with EGF with anti-EGFR (528) mAb or control IgG. Immune complexes were analyzed for the presence of tyrosine-phosphorylated GIV using anti-pY1764GIV and ligand-activated EGFR (pY1173 EGFR) by IB. (e) InsR was immunoprecipitated from lysates of Cos7 cells starved and stimulated with insulin with anti-pYInsR mAb. Immune complexes were analyzed for the presence of tyrosine phosphorylated GIV using anti-pY1764GIV and ligand-activated InsR (pYInsR) by IB.

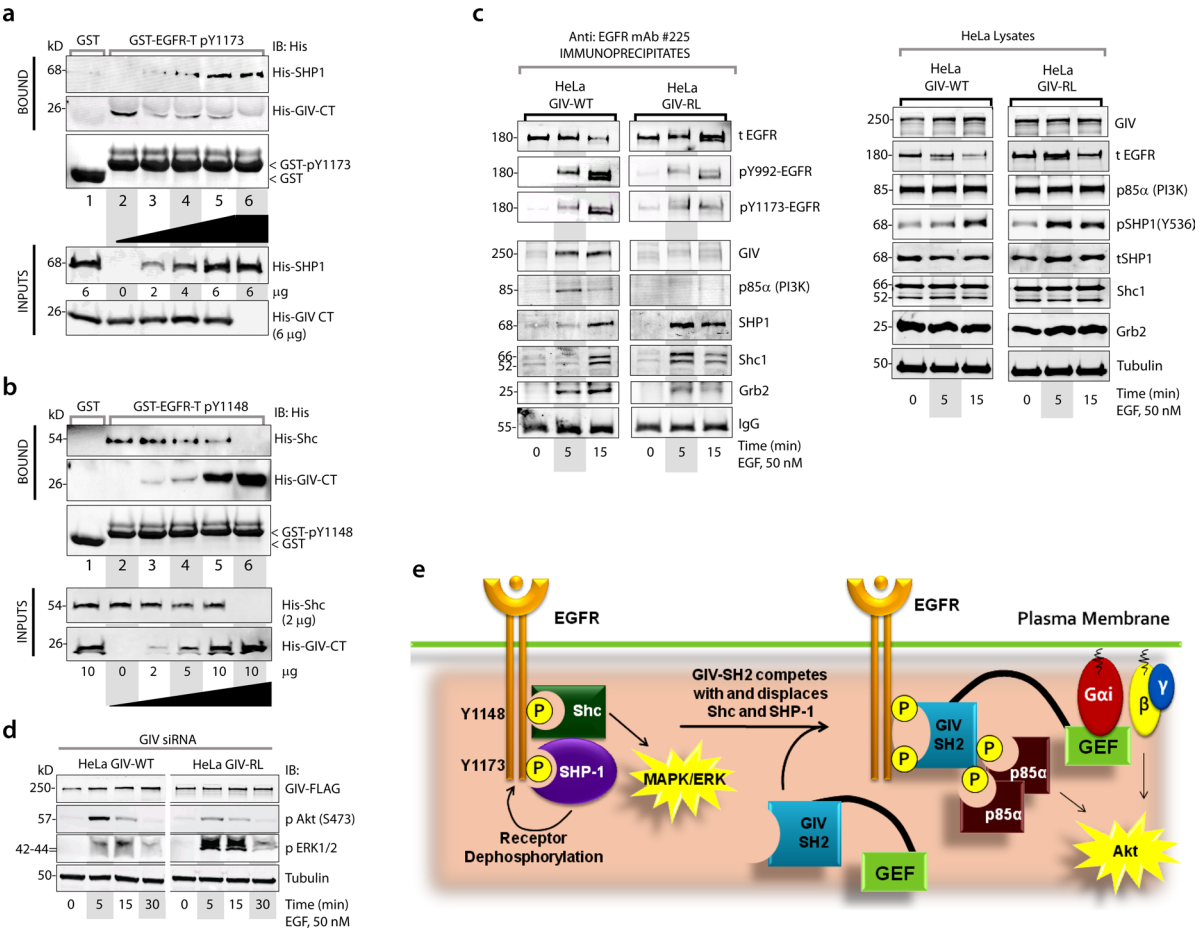

FIGURE 6: Interaction of GIV with EGFR determines the profile of other SH2 adaptors recruited to the ligand-activated receptor. (a) Equal aliquots (25 µg) of GST and GST-EGFR peptide containing Y1173 were autophosphorylated in vitro using recombinant EGFR kinase as in Figure 1c and subsequently used in pull-down assays with q constant amount (6 µg) of His-GIV-CT and increasing amounts of His-SHP-1 as indicated. Bound proteins were analyzed for His-SHP1 and His-GIV-CT by IB with His. (b) Equal aliquots (25 µg) of GST and GST-EGFR peptide containing Y1148 were autophosphorylated in vitro using recombinant EGFR kinase as in Figure 1c and subsequently used in pull-down assays with a constant amount (2 µg) of His-Shc1 and increasing amounts of His-GIV-CT as indicated. Bound proteins were analyzed for His-Shc1 and His-GIV-CT by IB with His. (c) HeLa GIV-WT and HeLa GIV-RL cells were depleted of endogenous GIV, starved, and stimulated with EGF as in Figure 4e before lysis. EGFR was immunoprecipitated from these lysates as in Figure 5d. Immunoprecipitates (left) and lysates (right) were analyzed for receptor phosphorylation and various SH2 adaptors by IB. Compared to HeLa GIV-WT cells, in HeLa GIV-RL cells, recruitment of SHP1 and Shc1 to ligand-activated EGFR is enhanced, autophosphorylation of EGFR is reduced, and recruitment of p85α (PI3K) and Grb2 is suppressed. (d) HeLa GIV-WT and HeLa GIV-RL cells were depleted of endogenous GIV, starved, and stimulated with EGF as in Figure 4e before lysis. Equal aliquots of whole-cell lysates were analyzed for phospho-Akt (pAkt), ERK (pERK1/2), and tubulin by IB. (e) Working model. A schematic summarizing the sequence of events triggered by the binding of GIV's SH2-like domain to EGFR. Left, in the absence of GIV, upon ligand stimulation, EGFR autophosphorylation is triggered at Y1148 and Y1173, which serve as sites of adaptor recruitment for Shc and SHP-1, respectively. Shc triggers activation of the MAPK/ERK pathway, and activated SHP-1 dephosphorylates EGFR and down-regulates receptor signaling. Right, in the presence of GIV, EGFR autophosphorylation sites pY1148 and pY1173 are recognized and approached by a partially structured SH2-like domain in GIV's C-terminus. Close proximity to EGFR facilitates efficient phosphorylation of GIV on critical tyrosines within a partially structured SH2 domain before/simultaneously with folding into a SH2-like module that stably docks onto autophosphorylated EGFR tail. Such docking competes with Shc for Y1148 and with SHP-1 for Y1173, thereby displacing and antagonizing signaling via both adaptors. Once GIV-SH2 is recruited to activated EGFR, GIV triggers two parallel pathways that were previously shown to synergistically activate Akt: a) GIV's phosphotyrosines bind p85α (class Ia PI3K) and activate PI3K/Akt signaling (Lin *et al.*, 2011), and b) GIV's GEF motif activates Gαi in close proximity to activated EGFR and releases "free" Gβγ, which directly binds p110 (class 1b PI3K) and activates PI3K/Akt signaling (Garcia-Marcos *et al.*, 2009).

GIV's SH2-like domain affects key events in EGFR activation and downstream signaling

We also demonstrate that besides linking Gi activation to RTKs, GIV's SH2-like domain has at least three other direct effects on growth factor signaling:

1) Recruitment of GIV to EGFR is required for enhancement of the PI3K/Akt signaling pathway after EGF stimulation. We previously showed that EGFR and other RTKs phosphorylate GIV on two tyrosines that directly bind and activate PI3K within RTK-GIV-PI3K complexes at the PM (Lin *et al.*, 2011), thereby serving as a bona

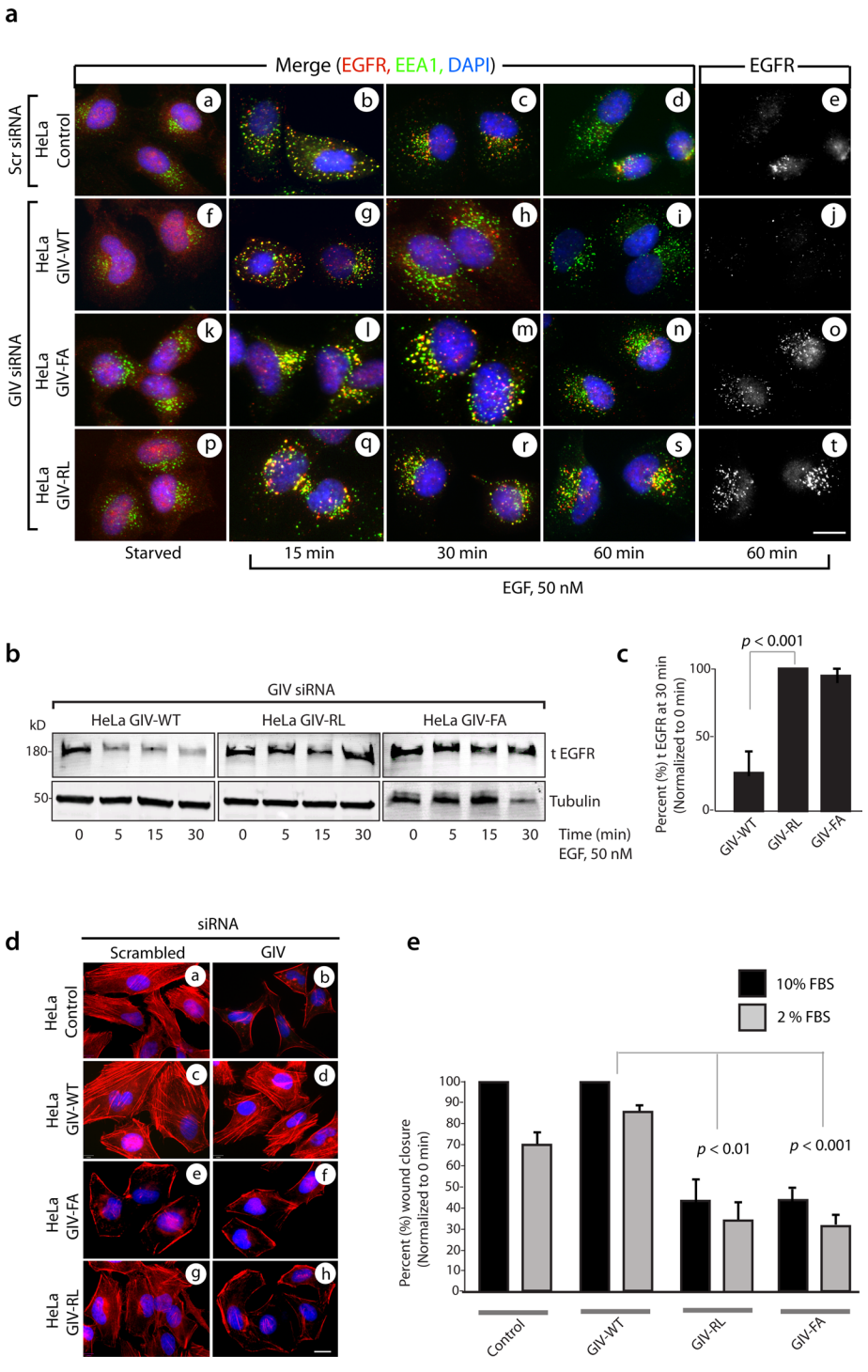

FIGURE 7: EGFR degradation is delayed and actin remodeling and cell migration are impaired in the absence of an intact SH2 domain in GIV. (a) HeLa control, HeLa GIV-WT, HeLa GIV-RL, and HeLa GIV-FA cells stably expressing siRNA-resistant GIV constructs were either treated with control (Scr) siRNA or GIV siRNA, starved, and stimulated with EGF as in Figure 4e before fixation. Cells were costained for EEA1 (green), tEGFR (red; anti-EGFR cytoplasmic tail), and the nucleus/DAPI (blue). At 60 min after ligand stimulation, EGFR is virtually undetectable in GIV-WT cells (e, j), but significant staining is seen in GIV-RL cells (t) compared with controls (e). Images are representative of four independent repeats. Bar, 10 µm. (b) Serum-starved control, GIV-WT, GIV-RL, and GIV-FA HeLa cells were stimulated with EGF as in a before lysis. Equal aliquots of lysates were analyzed for total EGFR (tEGFR, anti-EGFR cytoplasmic tail) and tubulin by immunoblotting. (c) The amount of tEGFR present at 30 min in b was quantified by Odyssey infrared imaging, normalized to tubulin, and expressed as percentage remaining compared with 0 min. Results are shown as mean ± SEM ($n = 4$). (d) Control HeLa cells or HeLa GIV-WT, GIV-FA, and GIV-RL cells expressing various siRNA-resistant GIV constructs were treated with scrambled or GIV siRNA as indicated. Fixed cells were costained with phalloidin–Texas red (F-actin, red) and DAPI (DNA, blue) and visualized by confocal microscopy. Stress fibers were reduced when endogenous GIV was depleted in control, HeLa GIV-FA (f), and HeLa GIV-RL (h) cells but not in HeLa GIV-WT cells. Both HeLa GIV-FA and GIV-RL cells show a paucity of stress fibers even without depletion of endogenous GIV (e, g), indicating that these GIV mutants have a dominant negative effect on actin remodeling. Bar, 10 µM. (e) HeLa control or HeLa GIV-WT and GIV-RL cells expressing various siRNA-resistant GIV constructs were treated with scrambled or GIV siRNA as in d. Cell migration was determined as described in *Materials and Methods*. Depletion of GIV inhibited migration in control and HeLa GIV-RL cells but not in HeLa GIV-WT cells.

fide enhancer of PI3K activity (Garcia-Marcos *et al.*, 2009; Lin *et al.*, 2011). Here we provide evidence that phosphorylation of GIV's C-terminal tyrosines by RTKs occurs when GIV exists in an intrinsically disordered state, because this phospho-event is inhibited once GIV is bound to its pTyr ligand and stably folded into a SH2-like module. We also show that upon phosphorylation, GIV folds/binds to ligand-activated RTKs. In cells expressing SH2-deficient GIV mutants, for which GIV is uncoupled from EGFR, tyrosine phosphorylation of GIV by EGFR is suppressed, recruitment of PI3K to EGFR-GIV complexes is decreased, and subsequent activation of downstream Akt kinase is diminished. On the basis of these findings, we propose that ligand-activated RTKs simultaneously induce two modifications on GIV: a) they trigger folding of an intrinsically disordered GIV C-terminus into a SH2-like domain, and b) they directly phosphorylate GIV's tyrosines. Our results indicate that initiation of folding and tyrosine phosphorylation must coincide, followed by completion of folding into a SH2-like domain that stably docks onto cytoplasmic tails of activated RTKs. Recruitment of tyrosine-phosphorylated GIV-SH2 to EGFR helps recruit and activate PI3K to initiate the previously defined 'RTK-GIV-PI3K' axis of signaling (Lin *et al.*, 2011).

2) We also demonstrate that recruitment of GIV to EGFR is required for suppression of the MAPK/ERK signaling pathway. Direct binding of GIV's SH2-like domain to pY1148 on EGFR tail competes with binding of Shc1, a major adaptor and a bona fide activator of Ras-MAPK/ERK signaling (Sakaguchi *et al.*, 1998). In cells

expressing SH2-deficient GIV mutants, for which GIV is uncoupled from EGFR, recruitment of Shc1 to EGFR and, consequently, downstream activation of ERK kinase are enhanced. We conclude that GIV suppresses the MAPK/ERK pathway in part by competitively inhibiting the recruitment of Shc1 to ligand-activated receptors.

3) Finally, we show that recruitment of GIV to EGFR is required for enhanced receptor autophosphorylation. We found that direct binding of GIV-SH2 to pY1173 on the EGFR tail competes with binding of SHP-1, which is a key protein tyrosine phosphatase (PTP) that dephosphorylates major autophosphorylation sites on EGFR tail (Okabayashi *et al.*, 1994). When GIV is uncoupled from EGFR in cells expressing SH2-deficient GIV, recruitment of SHP-1 to EGFR and subsequent tyrosine phosphorylation and activation of SHP-1 are enhanced, and the major autophosphorylation sites on EGFR are rapidly dephosphorylated. We conclude that GIV enhances receptor autophosphorylation in part by inhibiting the recruitment and subsequent activation of SHP-1. Because SHP-1 is also the major PTP that dephosphorylates GIV's tyrosines and antagonizes GIV-dependent PI3K activation (Mittal *et al.*, 2011), competitive inhibition of SHP-1 recruitment to EGFR-bound complexes at the PM may also delay dephosphorylation of GIV and further potentiate PI3K activation via the previously defined 'RTK-GIV-PI3K' axis of signaling.

Besides the aforementioned direct effects of GIV's interaction with EGFR, we also observe that binding of GIV to EGFR is required for rapid receptor transit through early endosomes and faster rates of receptor degradation. Because receptor signaling and trafficking are closely intertwined, it is possible that GIV's interaction with EGFR, which alters some of the earliest steps of receptor signaling at the PM, could directly or indirectly contribute to rapid down-regulation of EGFR through the endolysosomal pathway. Alternatively, it is possible that the formation of EGFR:GIV complexes on endosomes is required to link growth factor signaling to endosomal maturation (Beas *et al.*, 2012), a key determinant of the duration and strength of proliferative signaling from this compartment.

Together the foregoing findings provide mechanistic insights into our previously reported observations that GIV enhances EGFR autophosphorylation and motogenic (promigratory) PI3K/Akt signals but suppresses mitogenic MAPK/ERK signals after EGF stimulation, thereby orchestrating a signaling dichotomy (Ghosh *et al.*, 2010). We previously reported that such selective signal modulation allows GIV to skew the overall EGF signaling network in favor of persistent migration. Previous work predicted a central role for EGFR in creating such a dichotomy: EGFR autophosphorylation is essential for persistent cell migration but not for mitosis (Chen *et al.*, 1994a) and decisive signaling pathways that dictate whether cells migrate or divide diverge at the immediate postreceptor phase (Chen *et al.*, 1994b). Here we pinpointed the level of dichotomy as the EGFR:GIV interface assembled by GIV's SH2-like domain and the two phosphotyrosines on the EGFR tail. Such interaction, which mediates recruitment of GIV to EGFR, fundamentally alters the profile of adaptors recruited to the ligand-activated receptor and in that way shapes major downstream signaling pathways such that cells are biased to migrate.

GIV's SH2-like domain is an effective target to disengage GIV-dependent prometastatic signaling from multiple RTKs during cancer invasion

Because GIV serves as a bona fide enhancer of tumor invasion/metastasis in a variety of cancers, our results provide a unifying mechanism by which multiple oncogenic RTKs (IGF1R, EGFR, and VEGFR) modulate signals via GIV. On the basis of our findings in cells expressing the SH2-deficient GIV mutant, we conclude that the RTK:GIV interface and, more specifically, GIV's SH2-like domain are effective and attractive targets for antimetastatic therapy because of two outstanding reasons: 1) selective inhibition of this interaction effectively abolishes aberrant activation of PI3K downstream of multiple RTKs via GIV, promotes rapid dephosphorylation of receptor, and inhibits cell migration, indicating that this is a sensitive target; and 2) GIV's SH2-like domain is unique when compared with other known SH2 domains, in that the sequence similarity is weak despite similarities in folding and mechanism of phosphotyrosine recognition. Whereas most SH2 domains can be expressed in bacteria in the absence of phosphotyrosine ligands and have stable folding patterns identifiable by far-ultraviolet circular dichroism spectroscopy (Williams and Shoelson, 1993; Haan *et al.*, 1999; Arold *et al.*, 2001), GIV's SH2-like domain is intrinsically disordered in the resting state and folded exclusively after phosphotyrosine ligand binding. Multiple strategies for cloning and expressing GIV's ~110-aa-long SH2-like domain failed, each time yielding several breakdown products and little or no protein of expected size, although a larger C-terminus could be expressed in bacteria (in vitro pull-down assays) and the SH2-like domain alone could be expressed in mammalian cells (BiFC assays) as stable and functional products. This suggests that the isolated SH2-like domain of GIV, when expressed alone in bacteria, is disordered and unstable and may require ligand binding and/or flanking regions within GIV's C-terminus or other cellular proteins for folding and/or stability and functional integrity. We conclude that unlike most SH2 domains, GIV's SH2-like domain presents unique features that could provide specificity when targeting the GIV:RTK interface. Based on our findings, it is likely that use of small molecules against GIV-SH2 has the potential of being both selective and broad, selectively inhibiting GIV-dependent prometastatic growth factor signaling, yet acting broadly downstream of multiple RTKs.

Multimodular cooperation in GIV allows signal integration downstream of multiple RTKs via G protein intermediates

Besides this unique coexistence of GEF and SH2-like domains, GIV contains a growing list of many other of domains/motifs, cooperation between which could also be critical for its function as signal transducer (Figure 8). Here we demonstrated that GIV's GEF and SH2-like domains cooperate in the formation of RTK-GIV-Gαi ternary complexes and subsequent activation of Gαi. We also provided evidence that cooperation between GIV's SH2-like domain and its phosphotyrosines is essential for the formation of RTK-GIV-PI3K ternary complexes and subsequent activation of the PI3K/Akt pathway. That cells expressing SH2-deficient GIV mutants poorly remodel actin also suggests that SH2-like and actin-binding domains of GIV cooperate in linking EGF signaling to actin remodeling. It is likely that there are many more interdomain collaborations with the new discovered SH2-like domain—for example, the observed recruitment of GIV to the PM after growth factor stimulation is likely to be cooperatively mediated by its phosphatidylinositol 4-phosphate (PI4P) binding (Enomoto *et al.*, 2005) and the SH2 domains. The coiled-coil domain, which mediates homo-oligomerization (Enomoto *et al.*, 2005), could cooperate with the SH2-like domain to enhance clustering of RTK-GIV complexes at the PM. We propose that the SH2-like domain is key to achieve targeting and proximity of GIV to RTKs, which allows GIV to integrate incoming signals from these receptors and modulate them via activation of G proteins in the vicinity of the receptors. Examples of such interdomain collaborations were reported in the case of other multimodular signal transducers

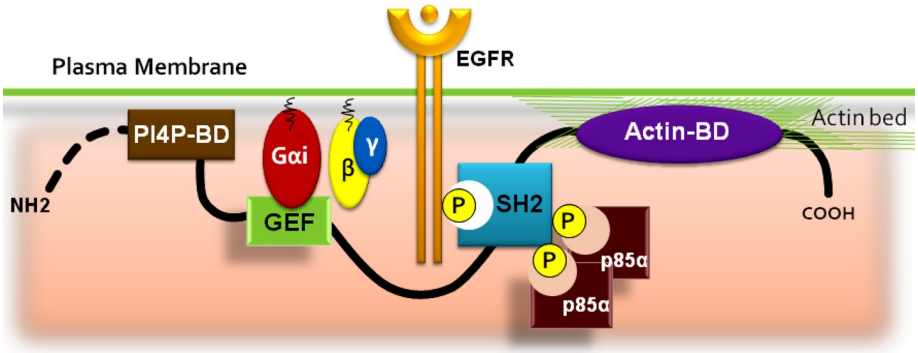

FIGURE 8: Multimodular cooperation allows GIV, a class 1 SH2-like adaptor, to link GEF activity for trimeric Gαi to cytoplasmic tails of ligand-activated RTKs. Schematic illustration of the modular structure of GIV from amino- to carboxyl-terminus: phosphoinositide-binding domain (PI4P-BD, brown), which binds membrane lipid and helps localize GIV to the PI4P-enriched plasma (PM), where ligand-activated receptors and G proteins are located; a GEF motif (green), which binds and activates Gαi; a SH2 domain (blue), which recognizes and docks onto the autophosphorylation sites on cytoplasmic tails of ligand-activated EGFR and other RTKs; a pair of phosphotyrosines (P), which directly bind p85α (PI3K) and activate class 1A PI3Ks; and an actin-binding domain (actin-BD, purple), which binds and remodels actin at the leading edge of migrating cells. These binding events cooperatively maintain GIV at the PM such that Gαi and PI3K are activated, and actin is remodeled in close proximity to RTKs. Recruitment of GIV-SH2 to RTKs and activation of Gαi in the vicinity of activated receptors enable GIV to modulate signaling programs downstream of the receptor. The plasticity of GIV's SH2-like domain between a stably folded and partially folded state is likely to regulate GIV's ability to engage with activated RTKs.

that bridge RTKs and small G proteins, such as Ras-GAP (Schlessinger and Lemmon, 2003), which inactivates Ras in the vicinity of ligand-activated receptors.

In conclusion, we defined a structural basis for how GIV, a nonreceptor GEF, forms a novel platform for activation of trimeric Gi proteins in the proximity of RTKs and helps define a new paradigm in signal transduction. The mechanistic and structural insights gained here not only characterize a new pharmacological target for uncoupling GIV from growth factor RTKs, they also shed light on the observed promiscuity and versatility of GIV as a signal transducer, that is, its ability to integrate signals downstream of multiple RTKs in a variety of cells during diverse cellular processes, such as cancer invasion, angiogenesis, epithelial wound healing, insulin response, cellular autophagy, and so on, all via G protein intermediates.

MATERIALS AND METHODS

Reagents and antibodies

Unless otherwise indicated, all reagents were of analytical grade and obtained from Sigma-Aldrich (St. Louis, MO). Cell culture media were purchased from Invitrogen (Carlsbad, CA). EGF and insulin were obtained from Invitrogen and Novagen, respectively. Recombinant EGFR (Millipore, Billerica, MA and Cell Signaling, Beverly, MA), VEGFR (Cell Signaling), and InsRβ (Sigma-Aldrich) were purchased from commercial sources. Recombinant His-Shc1 protein was purchased from Abnova (Taipei City, Taiwan). PP2 was obtained from Calbiochem. Silencer Negative Control scrambled (Scr) siRNA (Ghosh *et al.*, 2008) was purchased from Ambion (Grand Island, NY), and GIV siRNA (Garcia-Marcos *et al.*, 2009; Ghosh *et al.*, 2008, 2010) was custom ordered from Dharmacon (Lafayette, CO). Antibodies against GIV used in this work include rabbit serum and affinity-purified anti-GIV coiled-coil immunoglobulin G (IgG; GIV-ccAb; for immunoblotting only) raised against the coiled-coil domain of GIV (Garcia-Marcos *et al.*, 2009; Ghosh *et al.*, 2008, 2010) and affinity-purified anti-Girdin C-terminus (anti–GIV-CT, Girdin T-13; Santa Cruz Biotechnology, Dallas, TX; for immunoprecipitation) raised against the last 19 amino acids of the C-terminus of GIV. The anti-Gαi:GTP (6-F12) monoclonal antibody (mAb; Lane *et al.*, 2008) was a generous gift from Graeme Milligan (Glasgow, Scotland, UK, and subsequently commercially obtained from NewEast Biosciences (King of Prussia, PA). Total EGFR was visualized by immunofluorescence with mAb #225 raised against the ectodomain (a gift from Gordon Gill, University of California, San Diego, La Jolla, CA; Gill *et al.*, 1984) and by anti-EGFR polyclonal antibody (Santa Cruz Biotechnology) for immunoblotting. Rabbit monoclonal antibody against Tyr-1764-GIV was generated and validated in collaboration with Spring Biosciences (Pleasanton, CA) and Ventana (Tucson, AZ). Mouse monoclonal antibodies against phosphotyrosine (pTyr; 610000; BD Biosciences, San Jose, CA), FLAG (Sigma-Aldrich), polyhistidine (Sigma-Aldrich), phospho-Y845 EGFR (Millipore), hemagglutinin (HA; Covance, San Diego, CA), EEA1 (BD Biosciences), and tubulin (Sigma-Aldrich) were purchased from commercial sources. Rabbit polyclonal antibodies against FLAG (Invitrogen; for immunoblotting), GST (Santa Cruz Biotechnology), phospho-Y992 EGFR (Cell Signaling), total EGFR (Santa Cruz Biotechnology), Gαi3 (M-14; Santa Cruz Biotechnology), phospho-Akt S473 (Cell Signaling), pan-Gβ (Santa Cruz Biotechnology), and phospho-ERK 1/2 (Cell Signaling) were obtained commercially. Anti-mouse and anti-rabbit Alexa 594– and Alexa 488–coupled goat IgG for immunofluorescence and phalloidin were purchased from Invitrogen. Goat anti-rabbit and goat anti-mouse Alexa Fluor 680 or IRDye 800 F(ab')2 for immunoblotting were from Li-Cor Biosciences (Lincoln, NE). Control mouse and rabbit IgGs for immunoprecipitations were purchased from Bio-Rad (Hercules, CA) and Sigma-Aldrich, respectively.

Plasmid constructs and mutagenesis

Cloning of Gαi3 and GIV into pGEX-4T-1 or pET28b was described previously (Garcia-Marcos *et al.*, 2009). GST-EGFR-T (aa 1046–1210) was cloned into pGEX-4T-1 as described previously (Garcia-Marcos *et al.*, 2009). Various GST-EGFR tail peptides used in this work was generated by cloning fragments (amino acid boundaries indicated in Figure 1B) of human EGFR (GenBank accession number NM_005228; Protein ID NP_001529) into pGEX-4T-1 between *Bam*HI and *Eco*RI. The boundaries of each peptide were identified by the sequence flanking each tyrosine: Y1068 (YINQ), Y1086 (YHNQ), Y1114 (YLNT), Y1148 (YQQD), and Y1173 (YLRV). Hexahistidine (6-His)-tagged human SHP-1 PTP (GenBank accession number BC002523) cloned into pET28 expression vector was a generous gift from Richard Anderson (University of Wisconsin, Madison, WI; Bairstow *et al.*, 2005; Mittal *et al.*, 2011). Shc1 constructs were generous gifts from Tony Pawson (Mount Sinai Hospital, Toronto, Canada). For mammalian expression, C-terminal FLAG-tagged GIV was generated by cloning GIV into p3XFLAG-CMV-14 between *Not*I and *Bam*HI. RNA interference–resistant GIV was generated by silent mutations as described previously (Garcia-Marcos *et al.*, 2009). Insulin receptor-HA (Lin *et al.*, 2011)

was generated by cloning the human insulin receptor gene (GenBank accession number NM_000208) into pcDNA 3 (Invitrogen) and inserting a HA tag at the C-terminus. Purified His-Sec22 was a generous gift from Susan Ferro-Novick (University of California, San Diego, La Jolla, CA).

Multiple mutations on GIV used in this work were generated by site-directed mutagenesis using QuikChange kit (Stratagene, San Diego, CA) as per the manufacturer's protocols. All constructs were checked by DNA sequencing.

Protein expression and purification

All GST- and His-tagged constructs were expressed and purified from *Escherichia coli* strain BL21 (DE3; Invitrogen) as described previously (Garcia-Marcos *et al.*, 2009, 2010). Briefly, cultures of transformed bacteria were induced overnight at 25°C with 1 mM isopropyl β-D-1-thiogalactopyranoside, and a bacterial pellet from 1 l of culture was resuspended in 10 ml of GST-lysis buffer (25 mM Tris-HCl, pH 7.5, 20 mM NaCl, 1 mM EDTA, 20% [vol/vol] glycerol, 1% [vol/vol] Triton X-100, 2× protease inhibitor cocktail [Complete EDTA-free; Roche Diagnostics]) or His-lysis buffer (50 mM NaH_2PO_4, pH 7.4, 300 mM NaCl, 10 mM imidazole, 1% [vol/vol] Triton X-100, 2× protease inhibitor cocktail [Complete EDTA-free, Roche Diagnostics]) for GST- or His-fused proteins, respectively. After sonication (4 × 20 s, 1 min between cycles), lysates were centrifuged at 12,000 × *g* at 4°C for 20 min. Solubilized proteins were affinity purified on glutathione-Sepharose 4B beads (GE Healthcare) or HisPur Cobalt Resin (Pierce). Proteins were eluted, dialyzed overnight against phosphate-buffered saline (PBS), and stored at –80°C in aliquots. His-Gαi3 was buffer exchanged into G protein storage buffer (20 mM Tris-HCl, pH 7.4, 200 mM NaCl, 1 mM $MgCl_2$, 1 mM dithiothreitol [DTT], 10 μM GDP, 5% [vol/vol] glycerol) before storage at –80°C.

Generation of sequence alignment between GIV and 42 SH2 domains with resolved three-dimensional structures

Three-dimensional structures of 42 SH2 domains were retrieved from the Protein Data Bank (PBD; Rose *et al.*, 2011) and their corresponding amino acid sequences from UniProt Knowledgebase (www.uniprot.org/help/uniprotkb). The sequence alignment between these domains was built automatically using the Needleman and Wunsch algorithm with zero gap end penalties (ZEGA; Abagyan and Batalov, 1997), as implemented in ICM (Abagyan and Totrov, 1994; Abagyan *et al.*, 1994). The alignment was then adjusted manually with guidance from pairwise structural alignments of the 42 SH2 domains and subsequently modified to exclude the variable loops and retain only the conserved secondary structure elements of a canonical SH2 domain. The amino acid sequence of the human GIV C-terminus (BAE44387) was aligned against the obtained SH2 domain structure-sequence alignment by maximizing the total Gonnet comparison matrix score (Gonnet *et al.*, 1992) of the GIV sequence against all 42 sequences in the alignment while not allowing gaps in the conserved SH2 domain topological elements. The resulting alignment is shown in Supplemental Figure S1.

Construction of a three-dimensional model of the putative SH2 domains in the GIV C-terminus

A tentative model of GIV's C-terminal putative SH2 domain was constructed with the ICM homology modeling procedure (Abagyan *et al.*, 1997; Cardozo *et al.*, 1995, 2000) using the available structures of SH2 domains and the sequence alignment shown in Supplemental Figure S1. The conformation of the loops connecting the conserved secondary structure elements was obtained by a search in the library of PDB elements with similar terminus topology and sequence. Of all the models, the one based on the structure of human SOCS3-SH2 domain (PDB 2hmh) was chosen for further work because it had the lowest number of steric conflicts. The model was validated by generating a series of mutants that were predicted to decrease, increase, or have no effect on the phosphotyrosine-binding property of GIV-SH2 (Figure 3, a and b). Because of weak sequence similarity in the region of the αA helix, we could not computationally resolve an ambiguity in the alignment and conclusively state whether GIV K1722 or K1724 participates in coordination of the phosphorylated tyrosine on the substrate peptide. Consequently, both residues were mutated to better pinpoint how the pTyr-binding pocket is formed.

In vitro and in cellulo phosphorylation assays

In vitro kinase assays were performed using bacterially expressed GST-EGFR-tail peptides (~10–15 μg/reaction) and recombinant EGFR kinase. Reactions were started by adding 200–1000 μM ATP and carried out at 25°C for 60 min in tyrosine kinase buffer (60 mM 4-(2-hydroxyethyl)-1-piperazineethanesulfonic acid [HEPES], pH 7.5, 5 mM $MgCl_2$, 5 mM $MnCl_2$, 3 μM Na_3OV_4). Reactions were stopped by cooling to 4°C, and the phosphoprotein either was used in GST pull-down assays or analyzed by immunoblotting. For in cellulo phosphorylation assays on GIV-FLAG, assays were performed exactly as we did previously (Lin *et al.*, 2011). Briefly, FLAG-tagged GIV was coexpressed with untagged EGFR, and at 32 h after transfection, cells were starved for 16 h and preincubated with 100 μM sodium orthovanadate for 2 h and the Src inhibitor PP2 (250 nM) for 1 h before EGF (50 nM) stimulation, exactly as done previously (Lin *et al.*, 2011; Mittal *et al.*, 2011). Tyrosine phosphorylation was analyzed by immunoblotting using anti-pTyr mAb (BD Biosciences).

GST-pull-down assays

These assays were carried out as previously described (Ghosh *et al.*, 2010). Briefly, purified GST-fused EGFR peptides (15–35 μg) or GST alone (30–45 μg) were first phosphorylated by carrying out in vitro kinase assays with recombinant EGFR kinase (Invitrogen) and subsequently incubated for 2 h at 4°C in binding buffer (50 mM Tris-HCl, pH 7.4, 100 mM NaCl, 0.4% [vol/vol] NP-40, 10 mM $MgCl_2$, 5 mM EDTA, 2 mM DTT, and 2 mM sodium orthovanadate) containing WT or various mutants of His-GIV CT (aa 1660–1870). After 2 h, glutathione *S*-Sepharose beads (GE Healthcare) was added, and the incubation was carried out for another 4 h at 4°C with constant tumbling. The beads were then washed four times, each time with 1 ml of wash buffer (4.3 mM Na_2HPO_4, 1.4 mM KH_2PO_4, pH 7.4, 137 mM NaCl, 2.7 mM KCl, 0.1% [vol/vol] Tween-20, 10 mM $MgCl_2$, 5 mM EDTA, 2 mM DTT, and 2 mM sodium orthovanadate), and bound proteins were eluted in sample buffer for SDS–PAGE. When GST-Gαi3 was used in these assays, both binding and wash buffers were supplemented with 30 μM GDP. For His-pull-down assays with autophosphorylated RTKs, recombinant RTKs were first autophosphorylated by incubation in the presence of Mn and ATP exactly as in kinase assays (Lin *et al.*, 2011) and subsequent incubation with His-GIV-CT or His-Sec22 (negative control) proteins for 2 h at 4°C in binding buffer that was supplemented with 0.1 mg/ml bovine serum albumin (BSA) with constant tumbling. BSA-blocked His-Pur Cobalt beads (Pierce) were then added, and the incubation was carried out for another 4 h at 4°C.

Cell culture, transfection, lysis, and immunoprecipitation

Unless mentioned otherwise, cell lines used in this work were cultured according to American Type Culture Collection guidelines. Transfection was carried out using Genejuice (Novagen) for DNA

plasmids or Oligofectamine (Invitrogen) for siRNA oligos following the manufacturers' protocols, and stable cell lines were selected as mentioned previously (Garcia-Marcos *et al.*, 2009; Ghosh *et al.*, 2010) using the neomycin analogue G418 (Cellgro). HeLa cell lines stably expressing siRNA-resistant GIV-WT (HeLa-GIV-WT), GIV-F1685A mutant (HeLa-GIV-FA), and GIV-R1745L (HeLa-GIV-RL) were generated and maintained in the presence of G418 (500 µg/ml) as previously described (Ghosh *et al.*, 2010). Clones were chosen for each construct strictly so that they had relatively low abundance of exogenously expressed GIV (approximately one to two times the abundance of endogenous GIV), so that after depletion of the endogenous GIV protein by siRNA (for 48 h), each stable cell line expressed physiological levels of siRNA-resistant GIV-WT or mutant GIV constructs. For each construct, similar results were obtained from two separate clones.

Lysates for immunoprecipitation or pull-down assays were prepared by resuspending cells in lysis buffer (20 mM HEPES, pH 7.2, 5 mM Mg acetate, 125 mM K acetate, 0.4% Triton X-100, 1 mM DTT, supplemented with sodium orthovanadate [500 µM], phosphatase (Sigma-Aldrich), and protease [Roche] inhibitor cocktails), after which they were passed through a 30-gauge needle at 4°C and cleared (10,000–14,000 × *g* for 10 min) before use in subsequent experiments.

For immunoprecipitations, cell lysates (~1–2 mg of protein) were incubated for 4 h at 4°C with 2 µg of anti-FLAG mAb for immunoprecipitation of GIV-FLAG, anti-EGFR #225 mAb (Gill *et al.*, 1984) for endogenous EGFR, anti-HA mAb (Covance) for immunoprecipitation of HA-tagged insulin receptor, and control mouse IgGs where indicated. Protein G agarose beads (GE Healthcare) were added and incubated at 4°C for an additional 60 min. Beads were washed and then resuspended and boiled in SDS sample buffer. Buffers were supplemented with 1 mM sodium orthovanadate for all steps of the assay.

For immunoprecipitation of active Gαi3, freshly prepared cell lysates (2-4 mg) were incubated for 30 min at 4°C with the conformational Gαi3:GTP mouse antibody (1 µg; Lane *et al.*, 2008) or preimmune control mouse IgG. Protein G-Sepharose beads (GE Healthcare) were added and incubated at 4°C for additional 30 min (total duration of assay is 1 h). Beads were immediately washed three times using 1 ml of lysis buffer (composition exactly as before; no nucleotides added), and immune complexes were eluted by boiling in SDS as previously described (Ghosh *et al.*, 2010).

Steady-state GTPase assay

These assays were done as described previously (Garcia-Marcos *et al.*, 2009, 2010, 2011a, 2012). Briefly, 100 nM His-Gαi3 was preincubated with wild-type or R1745L mutant of His-GIV-CT (aa 1660–1870) for 15 min at 30°C in assay buffer (20 mM Na-HEPES, pH 8, 100 mM NaCl, 1 mM EDTA, 2 mM $MgCl_2$, 1 mM DTT, 0.05% [wt/vol] C12E10). GTPase reactions were initiated at 30°C by adding an equal volume of assay buffer containing 1 µM [γ-^{32}P]GTP (~50 cpm/fmol). Duplicate aliquots (50 µl) were removed at 10 min and reactions stopped with 950 µl of ice-cold 5% (wt/vol) activated charcoal in 20 mM H_3PO_4, pH 3. Samples were then centrifuged for 10 min at 10,000 × *g*, and 500 µl of the resultant supernatant was scintillation counted to quantify released [^{32}P]P_i. To determine the specific P_i produced, the background [^{32}P]P_i detected at 10 min in the absence of G protein was subtracted from each reaction. The results were expressed as relative to control (buffer, PBS, without GIV).

Measurement of cAMP

HeLa cells stably expressing GIV-WT or GIV-RL were depleted of endogenous GIV using siRNA, serum starved (0.2% fetal bovine serum [FBS], 16 h), and incubated with isobutylmethylxanthine (200 µM, 20 min), followed by EGF stimulation (50 nM, 20 min) and forskolin (10 µM, 10 min). To stop the reaction, cell medium was replaced with 150 µl of ice-cold trichloroacetic acid (TCA) 7.5% (wt/vol). cAMP content in TCA extracts was determined by radioimmunoassay (RIA). Production of cAMP was normalized to the amount of protein (determined using a dye-binding protein assay [Bio-Rad]) per sample (Ostrom *et al.*, 2001).

Immunofluorescence

These assays were done exactly as previously (Ghosh *et al.*, 2010; Garcia-Marcos *et al.*, 2011a), using a confocal Leica SPE microscope. To visualize all populations of receptors in cells, images were acquired as *Z*-stacks and maximally projected. Briefly, cells were fixed at room temperature with 3% paraformaldehyde for 20–25 min, permeabilized (0.2% Triton X-100) for 45 min, and incubated for 1 h each with primary and then secondary antibodies as described previously (Ghosh *et al.*, 2008). Antibody dilutions were as follows: mAb green fluorescent protein, 1:500; secondary goat anti-rabbit (594) and goat anti-mouse (488) Alexa-conjugated antibodies, 1:500; and 4′,6-diamidino-2-phenylindole (DAPI), 1:2000 (Molecular Probes). Samples were examined with a Leica SPE confocal microscope (Leica) using a 63× objective, and collected images were processed using ImageJ software (National Institutes of Health, Bethesda, MD) and assembled for presentation using Photoshop and Illustrator software (Adobe).

Bimolecular fluorescence complementation

Constructs used for BiFC assay were generated using Venus, a variant of YFP that contains a mutation to prevent dimerization (Nagai *et al.*, 2002). The C-terminus of Venus YFP (VC) was cloned into *Not*I and *Xho*I sites of a pcDNA3.1+ vector. This construct expresses 85 residues of the C-terminus Venus YFP, which also has a C-terminus HA tag. The N-terminus of Venus YFP (VN) was cloned into *Kpn*I and *Bam*HI sites of a pcDNA3.1+ vector. This construct expresses 173 residues of the N-terminus Venus YFP with a Myc tag. To generate VN-GIV SH2, aa 1714–1815 of human GIV was cloned into the *Bam*HI and *Not*I sites of the VN plasmid. Similarly, to generate EGFR-VC, human EGFR was cloned into the *Hin*dIII and *Not*I sites of VC plasmid. Venus N-terminus-tagged and C-terminus-tagged (VN and VC, respectively) constructs were cotransfected in various combinations using Genejuice (EMD Millipore) in Cos7 cells. Cells were maintained at steady state (10% FBS/DMEM), fixed, and stained at 36 h posttransfection with DAPI and imaged using a Leica SPE confocal microscope with a 63× objective. All constructs were expressed as a full-length protein without proteolysis/breakdown, as confirmed by full-length immunoblots.

Wound-healing assays

These assays were performed in the presence of serum exactly as described previously (Garcia-Marcos *et al.*, 2009; Ghosh *et al.*, 2010). Briefly, monolayers of HeLa cells were scratch-wounded with a 1-mm pipette tip, and multiple wound sites were serially photographed at 12-h intervals. Percentage wound closure was calculated by analyzing the wound area in the serial images, quantified using ImageJ.

Statistical analysis

Each experiment presented in the figures is representative of at least three independent experiments. Statistical significance (*p* value) between various conditions was assessed with the one-way analysis of variance (Bonferroni posthoc test). All graphical data presented were prepared using Prism software (GraphPad, La Jolla, CA).

ACKNOWLEDGMENTS

We thank Marilyn G. Farquhar for scientific advice and thoughtful comments during preparation of this article, Melanie Laederich and Yelena Pavlova for technical assistance with generation of constructs, Nakon Aroonsakool (all from the University of California, San Diego) for technical assistance with cAMP measurements, and scientists at Ventana and Spring Biosciences for help with generation and validation of pYGIV antibody. This work was funded by the National Institutes of Health (R01CA160911), the Burroughs Wellcome Fund, the Doris Duke Charitable Foundation, and the American Cancer Society (ACS-IRG 70-002) to P.G. K.M. was supported by a fellowship from the Susan G. Komen Foundation (SGK #PDF14298952); I.L.-S. by a fellowship from the American Heart Association (AHA #14POST20050025); and M.G-M. by Susan G. Komen Postdoctoral Fellowship KG080079 and the American Cancer Society (RGS-13-362-01-TBE); R.A. and I.K. were supported by National Institutes of Health Awards R01 GM071872, U01 GM094612, and U54 GM094618.

REFERENCES

Abagyan RA, Batalov S (1997). Do aligned sequences share the same fold? J Mol Biol 273, 355–368.

Abagyan R, Batalov S, Cardozo T, Totrov M, Webber J, Zhou Y (1997). Homology modeling with internal coordinate mechanics: deformation zone mapping and improvements of models via conformational search. Proteins Suppl 1, 29–37.

Abagyan R, Totrov M (1994). Biased probability Monte Carlo conformational searches and electrostatic calculations for peptides and proteins. J Mol Biol 235, 983–1002.

Abagyan R, Totrov M, Kuznetsov DA (1994). ICM: a new method for protein modeling and design: applications to docking and structure prediction from the distorted native conformation. J Comp Chem 15, 488–506.

Arold ST, Ulmer TS, Mulhern TD, Werner JM, Ladbury JE, Campbell ID, Noble ME (2001). The role of the Src homology 3-Src homology 2 interface in the regulation of Src kinases. J Biol Chem 276, 17199–17205.

Bairstow SF, Ling K, Anderson RA (2005). Phosphatidylinositol phosphate kinase type Igamma directly associates with and regulates Shp-1 tyrosine phosphatase. J Biol Chem 280, 23884–23891.

Batzer AG, Rotin D, Urena JM, Skolnik EY, Schlessinger J (1994). Hierarchy of binding sites for Grb2 and Shc on the epidermal growth factor receptor. Mol Cell Biol 14, 5192–5201.

Beas AO, Taupin V, Teodorof C, Nguyen LT, Garcia-Marcos M, Farquhar MG (2012). Galphas promotes EEA1 endosome maturation and shuts down proliferative signaling through interaction with GIV (Girdin). Mol Biol Cell 23, 4623–4634.

Cardozo T, Batalov S, Abagyan R (2000). Estimating local backbone structural deviation in homology models. Comput Chem 24, 13–31.

Cardozo T, Totrov M, Abagyan R (1995). Homology modeling by the ICM method. Proteins 23, 403–414.

Chen P, Gupta K, Wells A (1994a). Cell movement elicited by epidermal growth factor receptor requires kinase and autophosphorylation but is separable from mitogenesis. J Cell Biol 124, 547–555.

Chen P, Xie H, Sekar MC, Gupta K, Wells A (1994b). Epidermal growth factor receptor-mediated cell motility: phospholipase C activity is required, but mitogen-activated protein kinase activity is not sufficient for induced cell movement. J Cell Biol 127, 847–857.

Cismowski MJ, Ma C, Ribas C, Xie X, Spruyt M, Lizano JS, Lanier SM, Duzic E (2000). Activation of heterotrimeric G-protein signaling by a ras-related protein. Implications for signal integration. J Biol Chem 275, 23421–23424.

Cismowski MJ, Takesono A, Bernard ML, Duzic E, Lanier SM (2001). Receptor-independent activators of heterotrimeric G-proteins. Life Sci 68, 2301–2308.

Daub H, Weiss FU, Wallasch C, Ullrich A (1996). Role of transactivation of the EGF receptor in signalling by G-protein-coupled receptors. Nature 379, 557–560.

Decker SJ (1993). Transmembrane signaling by epidermal growth factor receptors lacking autophosphorylation sites. J Biol Chem 268, 9176–9179.

Dunker AK, Silman I, Uversky VN, Sussman JL (2008). Function and structure of inherently disordered proteins. Curr Opin Struct Biol 18, 756–764.

Dyson HJ, Wright PE (2002). Coupling of folding and binding for unstructured proteins. Curr Opin Struct Biol 12, 54–60.

Dyson HJ, Wright PE (2005). Intrinsically unstructured proteins and their functions. Nat Rev Mol Cell Biol 6, 197–208.

Enomoto A, Asai N, Namba T, Wang Y, Kato T, Tanaka M, Tatsumi H, Taya S, Tsuboi D, Kuroda K, *et al*. (2009). Roles of disrupted-in-schizophrenia 1-interacting protein girdin in postnatal development of the dentate gyrus. Neuron 63, 774–787.

Enomoto A, Murakami H, Asai N, Morone N, Watanabe T, Kawai K, Murakumo Y, Usukura J, Kaibuchi K, Takahashi M (2005). Akt/PKB regulates actin organization and cell motility via Girdin/APE. Dev Cell 9, 389–402.

Garcia-Marcos M, Ear J, Farquhar MG, Ghosh P (2011a). A GDI (AGS3) and a GEF (GIV) regulate autophagy by balancing G protein activity and growth factor signals. Mol Biol Cell 22, 673–686.

Garcia-Marcos M, Ghosh P, Ear J, Farquhar MG (2010). A structural determinant that renders G alpha(i) sensitive to activation by GIV/girdin is required to promote cell migration. J Biol Chem 285, 12765–12777.

Garcia-Marcos M, Ghosh P, Farquhar MG (2009). GIV is a nonreceptor GEF for G alpha i with a unique motif that regulates Akt signaling. Proc Natl Acad Sci USA 106, 3178–3183.

Garcia-Marcos M, Jung BH, Ear J, Cabrera B, Carethers JM, Ghosh P (2011b). Expression of GIV/Girdin, a metastasis-related protein, predicts patient survival in colon cancer. FASEB J 25, 590–599.

Garcia-Marcos M, Kietrsunthorn PS, Pavlova Y, Adia MA, Ghosh P, Farquhar MG (2012). Functional characterization of the guanine nucleotide exchange factor (GEF) motif of GIV protein reveals a threshold effect in signaling. Proc Natl Acad Sci USA 109, 1961–1966.

Ghosh P, Beas AO, Bornheimer SJ, Garcia-Marcos M, Forry EP, Johannson C, Ear J, Jung BH, Cabrera B, Carethers JM, *et al*. (2010). A Gαi-GIV molecular complex binds epidermal growth factor receptor and determines whether cells migrate or proliferate. Mol Biol Cell 21, 2338–2354.

Ghosh P, Garcia-Marcos M, Bornheimer SJ, Farquhar MG (2008). Activation of Galphai3 triggers cell migration via regulation of GIV. J Cell Biol 182, 381–393.

Ghosh P, Garcia-Marcos M, Farquhar MG (2011). GIV/Girdin is a rheostat that fine-tunes growth factor signals during tumor progression. Cell Adh Migr 5, 237–248.

Gill GN, Kawamoto T, Cochet C, Le A, Sato JD, Masui H, McLeod C, Mendelsohn J (1984). Monoclonal anti-epidermal growth factor receptor antibodies which are inhibitors of epidermal growth factor binding and antagonists of epidermal growth factor binding and antagonists of epidermal growth factor-stimulated tyrosine protein kinase activity. J Biol Chem 259, 7755–7760.

Gonnet GH, Cohen MA, Benner SA (1992). Exhaustive matching of the entire protein sequence database. Science 256, 1443–1445.

Gschwind A, Fischer OM, Ullrich A (2004). The discovery of receptor tyrosine kinases: targets for cancer therapy. Nat Rev Cancer 4, 361–370.

Haan S, Hemmann U, Hassiepen U, Schaper F, Schneider-Mergener J, Wollmer A, Heinrich PC, Grotzinger J (1999). Characterization and binding specificity of the monomeric STAT3-SH2 domain. J Biol Chem 274, 1342–1348.

Helin K, Velu T, Martin P, Vass WC, Allevato G, Lowy DR, Beguinot L (1991). The biological activity of the human epidermal growth factor receptor is positively regulated by its C-terminal tyrosines. Oncogene 6, 825–832.

Iakoucheva LM, Brown CJ, Lawson JD, Obradovic Z, Dunker AK (2002). Intrinsic disorder in cell-signaling and cancer-associated proteins. J Mol Biol 323, 573–584.

Iakoucheva LM, Radivojac P, Brown CJ, O'Connor TR, Sikes JG, Obradovic Z, Dunker AK (2004). The importance of intrinsic disorder for protein phosphorylation. Nucleic Acids Res 32, 1037–1049.

Jiang P, Enomoto A, Jijiwa M, Kato T, Hasegawa T, Ishida M, Sato T, Asai N, Murakumo Y, Takahashi M (2008). An actin-binding protein Girdin regulates the motility of breast cancer cells. Cancer Res 68, 1310–1318.

Keilhack H, Tenev T, Nyakatura E, Godovac-Zimmermann J, Nielsen L, Seedorf K, Bohmer FD (1998). Phosphotyrosine 1173 mediates binding of the protein-tyrosine phosphatase SHP-1 to the epidermal growth factor receptor and attenuation of receptor signaling. J Biol Chem 273, 24839–24846.

Kitamura T, Asai N, Enomoto A, Maeda K, Kato T, Ishida M, Jiang P, Watanabe T, Usukura J, Kondo T, *et al*. (2008). Regulation of VEGF-mediated angiogenesis by the Akt/PKB substrate Girdin. Nat Cell Biol 10, 329–337.

Lane JR, Henderson D, Powney B, Wise A, Rees S, Daniels D, Plumpton C, Kinghorn I, Milligan G (2008). Antibodies that identify only the active conformation of G(i) family G protein alpha subunits. FASEB J 22, 1924–1932.
Lee MJ, Dohlman HG (2008). Coactivation of G protein signaling by cell-surface receptors and an intracellular exchange factor. Curr Biol 18, 211–215.
Liebmann C, Bohmer FD (2000). Signal transduction pathways of G protein-coupled receptors and their cross-talk with receptor tyrosine kinases: lessons from bradykinin signaling. Curr Med Chem 7, 911–943.
Lin C, Ear J, Pavlova Y, Mittal Y, Kufareva I, Ghassemian M, Abagyan R, Garcia-Marcos M, Ghosh P (2011). Tyrosine phosphorylation of the Galpha-interacting protein GIV promotes activation of phosphoinositide 3-kinase during cell migration. Sci Signal 4, ra64.
Liu BA, Shah E, Jablonowski K, Stergachis A, Engelmann B, Nash PD (2011). The SH2 domain-containing proteins in 21 species establish the provenance and scope of phosphotyrosine signaling in eukaryotes. Sci Signal 4, ra83.
Lopez-Sanchez I, Dunkel Y, Roh YS, Mittal Y, De Minicis S, Muranyi A, Singh S, Shanmugam K, Aroonsakool N, Murray F, *et al.* (2014). GIV/Girdin is a central hub for profibrogenic signalling networks during liver fibrosis. Nat Commun 5, 4451.
Lowes VL, Ip NY, Wong YH (2002). Integration of signals from receptor tyrosine kinases and g protein-coupled receptors. Neuro-Signals 11, 5–19.
Luttrell LM (2006). Transmembrane signaling by G protein-coupled receptors. Methods Mol Biol 332, 3–49.
Luttrell LM, Daaka Y, Lefkowitz RJ (1999). Regulation of tyrosine kinase cascades by G-protein-coupled receptors. Curr Opin Cell Biol 11, 177–183.
Margolis BL, Lax I, Kris R, Dombalagian M, Honegger AM, Howk R, Givol D, Ullrich A, Schlessinger J (1989). All autophosphorylation sites of epidermal growth factor (EGF) receptor and HER2/neu are located in their carboxyl-terminal tails. Identification of a novel site in EGF receptor. J Biol Chem 264, 10667–10671.
Marinissen MJ, Gutkind JS (2001). G-protein-coupled receptors and signaling networks: emerging paradigms. Trends Pharmacol Sci 22, 368–376.
Marty C, Ye RD (2010). Heterotrimeric G protein signaling outside the realm of seven transmembrane domain receptors. Mol Pharmacol 78, 12–18.
Mills GB, Moolenaar WH (2003). The emerging role of lysophosphatidic acid in cancer. Nat Rev 3, 582–591.
Mittal Y, Pavlova Y, Garcia-Marcos M, Ghosh P (2011). Src homology domain 2-containing protein-tyrosine phosphatase-1 (SHP-1) binds and dephosphorylates G(alpha)-interacting, vesicle-associated protein (GIV)/Girdin and attenuates the GIV-phosphatidylinositol 3-kinase (PI3K)-Akt signaling pathway. J Biol Chem 286, 32404–32415.
Miyake H, Maeda K, Asai N, Shibata R, Ichimiya H, Isotani-Sakakibara M, Yamamura Y, Kato K, Enomoto A, Takahashi M, *et al.* (2011). The actin-binding protein Girdin and its Akt-mediated phosphorylation regulate neointima formation after vascular injury. Circ Res 108, 1170–1179.
Nagai T, Ibata K, Park ES, Kubota M, Mikoshiba K, Miyawaki A (2002). A variant of yellow fluorescent protein with fast and efficient maturation for cell-biological applications. Nat Biotechnol 20, 87–90.
Natarajan K, Berk BC (2006). Crosstalk coregulation mechanisms of G protein-coupled receptors and receptor tyrosine kinases. Methods Mol Biol 332, 51–77.
Okabayashi Y, Kido Y, Okutani T, Sugimoto Y, Sakaguchi K, Kasuga M (1994). Tyrosines 1148 and 1173 of activated human epidermal growth factor receptors are binding sites of Shc in intact cells. J Biol Chem 269, 18674–18678.
Okutani T, Okabayashi Y, Kido Y, Sugimoto Y, Sakaguchi K, Matuoka K, Takenawa T, Kasuga M (1994). Grb2/Ash binds directly to tyrosines 1068 and 1086 and indirectly to tyrosine 1148 of activated human epidermal growth factor receptors in intact cells. J Biol Chem 269, 31310–31314.
Ostrom RS, Gregorian C, Drenan RM, Xiang Y, Regan JW, Insel PA (2001). Receptor number and caveolar co-localization determine receptor coupling efficiency to adenylyl cyclase. J Biol Chem 276, 42063–42069.
Piiper A, Zeuzem S (2004). Receptor tyrosine kinases are signaling intermediates of G protein-coupled receptors. Curr Pharm Des 10, 3539–3545.
Poppleton H, Sun H, Fulgham D, Bertics P, Patel TB (1996). Activation of Gsalpha by the epidermal growth factor receptor involves phosphorylation. J Biol Chem 271, 6947–6951.
Porteous D, Millar K (2009). How DISC1 regulates postnatal brain development: girdin gets in on the AKT. Neuron 63, 711–713.
Puseenam A, Yoshioka Y, Nagai R, Hashimoto R, Suyari O, Itoh M, Enomoto A, Takahashi M, Yamaguchi M (2009). A novel Drosophila Girdin-like protein is involved in Akt pathway control of cell size. Exp Cell Res 315, 3370–3380.
Rose PW, Beran B, Bi C, Bluhm WF, Dimitropoulos D, Goodsell DS, Prlic A, Quesada M, Quinn GB, Westbrook JD, *et al.* (2011). The RCSB Protein Data Bank: redesigned web site and web services. Nucleic Acids Res 39, D392–D401.
Sakaguchi K, Okabayashi Y, Kido Y, Kimura S, Matsumura Y, Inushima K, Kasuga M (1998). Shc phosphotyrosine-binding domain dominantly interacts with epidermal growth factor receptors and mediates Ras activation in intact cells. Mol Endocrinol 12, 536–543.
Savage CR Jr, Cohen S (1972). Epidermal growth factor and a new derivative. Rapid isolation procedures and biological and chemical characterization. J Biol Chem 247, 7609–7611.
Schafer B, Gschwind A, Ullrich A (2004). Multiple G-protein-coupled receptor signals converge on the epidermal growth factor receptor to promote migration and invasion. Oncogene 23, 991–999.
Schlessinger J (1994). SH2/SH3 signaling proteins. Curr Opin Genet Dev 4, 25–30.
Schlessinger J, Lemmon MA (2003). SH2 and PTB domains in tyrosine kinase signaling. Sci STKE 2003 RE12.
Shyu YJ, Suarez CD, Hu CD (2008). Visualization of ternary complexes in living cells by using a BiFC-based FRET assay. Nat Protocols 3, 1693–1702.
Siderovski DP, Willard FS (2005). The GAPs, GEFs, and GDIs of heterotrimeric G-protein alpha subunits. Int J Biol Sci 1, 51–66.
Songyang Z, Shoelson SE, Chaudhuri M, Gish G, Pawson T, Haser WG, King F, Roberts T, Ratnofsky S, Lechleider RJ, *et al.* (1993). SH2 domains recognize specific phosphopeptide sequences. Cell 72, 767–778.
Songyang Z, Shoelson SE, McGlade J, Olivier P, Pawson T, Bustelo XR, Barbacid M, Sabe H, Hanafusa H, Yi T, *et al.* (1994). Specific motifs recognized by the SH2 domains of Csk, 3BP2, fps/fes, GRB-2, HCP, SHC, Syk, and Vav. Mol Cell Biol 14, 2777–2785.
Sorkin A, Helin K, Waters CM, Carpenter G, Beguinot L (1992). Multiple autophosphorylation sites of the epidermal growth factor receptor are essential for receptor kinase activity and internalization. Contrasting significance of tyrosine 992 in the native and truncated receptors. J Biol Chem 267, 8672–8678.
Sorkin A, Waters C, Overholser KA, Carpenter G (1991). Multiple autophosphorylation site mutations of the epidermal growth factor receptor. Analysis of kinase activity and endocytosis. J Biol Chem 266, 8355–8362.
Sun H, Seyer JM, Patel TB (1995). A region in the cytosolic domain of the epidermal growth factor receptor antithetically regulates the stimulatory and inhibitory guanine nucleotide-binding regulatory proteins of adenylyl cyclase. Proc Natl Acad Sci USA 92, 2229–2233.
Tall GG, Krumins AM, Gilman AG (2003). Mammalian Ric-8A (synembryn) is a heterotrimeric Galpha protein guanine nucleotide exchange factor. J Biol Chem 278, 8356–8362.
Walton GM, Chen WS, Rosenfeld MG, Gill GN (1990). Analysis of deletions of the carboxyl terminus of the epidermal growth factor receptor reveals self-phosphorylation at tyrosine 992 and enhanced in vivo tyrosine phosphorylation of cell substrates. J Biol Chem 265, 1750–1754.
Wang Y, Kaneko N, Asai N, Enomoto A, Isotani-Sakakibara M, Kato T, Asai M, Murakumo Y, Ota H, Hikita T, *et al.* (2011). Girdin is an intrinsic regulator of neuroblast chain migration in the rostral migratory stream of the postnatal brain. J Neurosci 31, 8109–8122.
Wang H, Misaki T, Taupin V, Eguchi A, Ghosh P, Farquhar MG (2014). GIV/Girdin links vascular endothelial growth factor signaling to Akt survival signaling in podocytes independent of nephrin. J Am Soc Nephrol, ASN.2013090985.
Williams KP, Shoelson SE (1993). Cooperative self-assembly of SH2 domain fragments restores phosphopeptide binding. Biochemistry 32, 11279–11284.
Yamaguchi M, Suyari O, Nagai R, Takahashi M (2010). dGirdin a new player of Akt /PKB signaling in Drosophila melanogaster. Front Biosci 15, 1164–1171.